doi:10.1093/brain/aws275 Brain 2012: 135; 3567–3583 | 3567

BRAIN
A JOURNAL OF NEUROLOGY

Myelin is dependent on the Charcot–Marie–Tooth Type 4H disease culprit protein FRABIN/FGD4 in Schwann cells

Michael Horn,[1] Reto Baumann,[1,*] Jorge A. Pereira,[1,*] Páris N. M. Sidiropoulos,[1,*] Christian Somandin,[1,*] Hans Welzl,[2] Claudia Stendel,[1,†] Tessa Lühmann,[3,‡] Carsten Wessig,[4] Klaus V. Toyka,[4,§] João B. Relvas,[1,5] Jan Senderek[1,¶] and Ueli Suter[1]

1 Department of Biology, Institute of Molecular Health Sciences, Cell Biology, Swiss Federal Institute of Technology, ETH Zurich, 8093 Zurich, Switzerland
2 Division of Neuroanatomy and Behaviour, Institute of Anatomy, University of Zürich, Winterthurerstrasse 190, 8057 Zürich, Switzerland
3 Laboratory for Biologically Oriented Materials, Department of Materials, Swiss Federal Institute of Technology, ETH Zurich, 8093 Zurich, Switzerland
4 Department of Neurology, University of Würzburg, 97080 Würzburg, Germany
5 Instituto de Biologia Molecular e Celular, Universidade do Porto, 4150-180 Porto, Portugal

* These authors contributed equally to this work (listed alphabetically)

† Present address: Department of Neurology, Rheinisch Westfälische Technische Hochschule (RWTH) Aachen, 52074 Aachen, Germany

‡ Present address: Institute for Pharmacy and Food Chemistry, University of Würzburg, Am Hubland, 97074 Würzburg, Germany

§ Present address: Department of Physiology – Neurophysiology, University of Würzburg, 97080 Würzburg, Germany

¶ Present address: Department of Neurology, Friedrich-Baur Institute, Ludwig-Maximilian University, 80336 Munich, Germany

Correspondence to: Dr. Ueli Suter,
Institute of Molecular Health Sciences,
ETH-Hönggerberg,
CH-8093 Zürich,
Switzerland
E-mail: ueli.suter@cell.biol.ethz.ch

Studying the function and malfunction of genes and proteins associated with inherited forms of peripheral neuropathies has provided multiple clues to our understanding of myelinated nerves in health and disease. Here, we have generated a mouse model for the peripheral neuropathy Charcot–Marie–Tooth disease type 4H by constitutively disrupting the mouse orthologue of the suspected culprit gene *FGD4* that encodes the small RhoGTPase Cdc42-guanine nucleotide exchange factor Frabin. Lack of Frabin/Fgd4 causes dysmyelination in mice in early peripheral nerve development, followed by profound myelin abnormalities and demyelination at later stages. At the age of 60 weeks, this was accompanied by electrophysiological deficits. By crossing mice carrying alleles of Frabin/*Fgd4* flanked by loxP sequences with animals expressing Cre recombinase in a cell type-specific manner, we show that Schwann cell-autonomous Frabin/Fgd4 function is essential for proper myelination without detectable primary contributions from neurons. Deletion of Frabin/Fgd4 in Schwann cells of fully myelinated nerve fibres revealed that this protein is not only required for correct nerve development but also for accurate myelin maintenance. Moreover, we established that correct activation of Cdc42 is dependent on Frabin/Fgd4 function in healthy peripheral nerves. Genetic disruption of Cdc42 in Schwann cells of adult myelinated nerves resulted in myelin alterations similar to those observed in Frabin/Fgd4-deficient mice, indicating that Cdc42 and the Frabin/Fgd4–Cdc42 axis are critical for myelin homeostasis. In line with known regulatory

Received June 8, 2012. Revised July 24, 2012. Accepted August 15, 2012

roles of Cdc42, we found that Frabin/Fgd4 regulates Schwann cell endocytosis, a process that is increasingly recognized as a relevant mechanism in peripheral nerve pathophysiology. Taken together, our results indicate that regulation of Cdc42 by Frabin/Fgd4 in Schwann cells is critical for the structure and function of the peripheral nervous system. In particular, this regulatory link is continuously required in adult fully myelinated nerve fibres. Thus, mechanisms regulated by Frabin/Fgd4–Cdc42 are promising targets that can help to identify additional regulators of myelin development and homeostasis, which may crucially contribute also to malfunctions in different types of peripheral neuropathies.

Keywords: Charcot–Marie–Tooth disease; hereditary motor and sensory neuropathy; myelination; Rho-GTPase Cdc42; Frabin/Fgd4

Abbreviations: Dlg1 = disc large homologue 1; GEF = guanine nucleotide exchange factor; PTEN = phosphatase and tensin homologue

Introduction

Charcot–Marie–Tooth disease, also known as hereditary motor and sensory neuropathy, is one of the most common inherited neurological disorders (Skre, 1974). Charcot–Marie–Tooth disease is a clinically and genetically heterogenous disease, usually characterized by distal muscle weakness and atrophy, distal sensory loss and limb deformities (Shy *et al.*, 2005). Clinically, Charcot–Marie–Tooth disease is divided based on electrophysiological and histopathological characteristics into demyelinating or dysmyelinating (CMT1, CMT3 and CMT4) and axonal forms (CMT2). The demyelinating or dysmyelinating neuropathies are commonly assumed to start with damage to Schwann cells and are mainly associated with reduced nerve conduction velocity. However, as demyelinating Charcot–Marie–Tooth disease progresses and axonal degeneration becomes an additional pathological feature, reduced amplitudes and dispersion of compound muscle action potentials become the main correlate to clinical disability (Krajewski *et al.*, 2000; Suter and Scherer, 2003). Axonal forms of Charcot–Marie–Tooth disease are thought to originate on the neuronal side and are linked to decreased compound muscle action potential amplitudes. The distinction with regard to the initially affected cell type is blurred in intermediate forms of Charcot–Marie–Tooth disease (Nicholson and Myers, 2006). As was recently shown, neuron-specific ablation of the prion protein in mice may cause a demyelinating neuropathy (Bremer *et al.*, 2010). This observation reiterated that experimental proof is required to unambiguously determine the originally affected cell type(s) in peripheral neuropathies, as peripheral nerves are controlled by continuous reciprocal Schwann cell–neuron interactions (Nave, 2010; Pereira *et al.*, 2012). Such knowledge is critical to understand the underlying disease mechanisms in the different forms of Charcot–Marie–Tooth disease and provides a rational basis for potential treatment strategies.

Mutations in >30 genes are associated with Charcot–Marie–Tooth disease variants, with autosomal dominant, autosomal recessive or X-linked inheritance patterns (Reilly *et al.*, 2011). The subtype CMT4H belongs to the autosomal recessive demyelinating forms of Charcot–Marie–Tooth disease (De Sandre-Giovannoli *et al.*, 2005). Several different mutations in FRABIN/*FGD4*, a member of a family of Cdc42-specific guanine nucleotide exchange factors (GEFs) (Nakanishi and Takai, 2008), have been associated with CMT4H (Delague *et al.*, 2007; Stendel *et al.*, 2007; Fabrizi *et al.*, 2009; Houlden *et al.*, 2009). These include missense, nonsense, frame-shifting and splice mutations. The relatively small number of patients does not allow a well-founded genotype–phenotype correlation. Generally, patients with the CMT4H subtype are clinically affected in early childhood, with disease onset occasionally as early as the first year of life (Baets *et al.*, 2011). In most cases, CMT4H is characterized by a slowly progressive neuropathy with increasing distal sensory loss and distal weakness. Electrophysiological examinations revealed markedly reduced nerve conduction velocity. Nerve biopsies show redundant myelin and myelin infoldings and outfoldings as striking pathological hallmarks. Furthermore, severely hypomyelinated fibres indicate demyelination and remyelination consistent with the classification of CMT4H as demyelinating Charcot–Marie–Tooth disease (De Sandre-Giovannoli *et al.*, 2005; Stendel *et al.*, 2007; Fabrizi *et al.*, 2009). Reduced density of myelinated large calibre fibres, likely caused by axonal degeneration, appears as an additional feature.

The available knowledge from human genetics suggests a strict dependence of myelinated peripheral nerves on Frabin/Fgd4. However, the current information concerning Frabin/Fgd4 function is limited and has been obtained from cell culture studies in mainly non-neural cells (Nakanishi and Takai, 2008). We wished to examine Frabin/Fgd4 function *in vivo*. For this purpose, we used mouse genetics focusing on nerve development and nerve homeostasis. We reasoned that these experiments would also be instrumental for our understanding of the disease mechanism involved in CMT4H and related neuropathies. Our analysis led to the establishment of an animal model for CMT4H and revealed that Schwann cells are the main cell type initially affected by the loss of Frabin/Fgd4 function. Furthermore, we found that the critical role of Frabin/Fgd4 in peripheral nerves is linked to its molecular function as GEF for Cdc42 and most likely involves regulation of endocytosis.

Materials and methods

Mice

Frabin mutant mice were produced by standard technology (Mouse Clinical Institute, Strasbourg, France). Cdc42 mutants (Thurnherr *et al.*, 2006; Wu *et al.*, 2006; Benninger *et al.*, 2007), Hb9-Cre (Arber *et al.*, 1999) and Dhh-Cre (Jaegle *et al.*, 2003; Pereira *et al.*, 2009) mice

have been described. In experiments involving the Plp-CreERT2 transgene (Leone *et al.*, 2003), Cre recombinase was activated by repeated injection of tamoxifen (100 mg/kg, intraperitoneally) in 10-week-old mice on 5 consecutive days. Genotypes of mice were determined by PCR on genomic DNA derived from ear biopsies using appropriate primer pairs (Supplementary material). Mice were kept under standard housing conditions on Lignocel bedding (Provimi). Experiments followed approved protocols (Veterinary Office, Canton Zurich, Switzerland).

Behavioural analysis

SHIRPA (SmithKline, Harwell, Imperial College, Royal London Hospital, phenotype assessment) was carried out as described (Rogers *et al.*, 1997). Sensory and motor tests followed established protocols (Bremer *et al.*, 2010).

Electrophysiology

Motor nerve conduction in 30- and 60-week-old anaesthetized mice was measured as described (Zielasek *et al.*, 1996; Bremer *et al.*, 2010). In brief, upon supramaximal stimulation (i.e. at least 30% above the current needed to obtain a maximal compound muscle action potential) of the tibial nerve at the ankle ('distal') and stimulation of the sciatic nerve at the sciatic notch ('proximal'), compound muscle action potentials were recorded with a pair of steel needle electrodes in the foot muscles. Nerve conduction velocities were calculated in metres per second from distal and proximal latencies. Ten successive F-waves were recorded, and the shortest latencies were taken upon stimulation at the ankle (Zielasek *et al.*, 1996).

Electron microscopy and histological analysis

Tissue embedding and electron microscopy were performed as described (Pereira *et al.*, 2010; Somandin *et al.*, 2012). Ultrathin sections were collected on carbon-coated Formvar grids (Electron Microscopy Sciences) and analysed in a Morgagni 268 transmission electron microscope. Complete transverse sections of plantaris, quadriceps and saphenous nerves were captured at $\times 1000$ magnification and were reconstructed using Adobe® Photoshop®. All affected fibres carrying aberrant myelin features were quantified per nerve section. Myelin thickness was measured in Adobe® Photoshop® on electron microscopy pictures.

RhoGTPase activity assay

Cdc42 activity was measured as described (Sander *et al.*, 1998; Benninger *et al.*, 2007). The glutathione-*S*-transferase–p21-activated kinase–crib (Cdc42–Rac1 interactive binding) domain construct was provided by Dr J. Collard (The Netherlands Cancer Institute, Amsterdam). In brief, the material to be analysed (sciatic nerves or Schwann cells) was homogenized in 10% glycerol, 50 mM Tris–HCl, pH 7.4, 100 mM NaCl, 1% Nonidet P-40, 2 mM $MgCl_2$ and protease inhibitor cocktail (Sigma-Aldrich) and was centrifuged for 5 min at 21 000*g* at 4°C. Aliquots of 10% of the volume were taken from the supernatant to determine the total protein amount. The remaining supernatant was incubated with the bait protein bound to glutathione-coupled Sepharose™ beads (GE Healthcare) at 4°C for 60 min. The beads and protein bound to the fusion protein were washed three times in an excess of homogenization buffer, eluted in Laemmli sample buffer and analysed for bound Cdc42 by western blotting.

Cell culture and expression silencing

RT4 rat schwannoma cells were grown in Dulbecco's modified Eagle's medium containing 10% foetal calf serum (Gibco) and were transfected using Lipofectamine® 2000 (Invitrogen) according to the manufacturer's protocol. Small interfering RNA transfections were carried out repeatedly at 72, 48 and 24 h before assays were performed. Frabin/Fgd4 expression silencing: Fgd4 small interfering RNA (SI01512574; Qiagen) with the targeting sequence 5′-CTG AAT GGA GTA AGA AAC GAA-3′. Control small interfering RNA: AllStars Negative Control siRNA (1027292; Qiagen). For fluorescence-activated flow cytometry and microscopy analysis, small interfering RNAs were labelled with Alexa Fluor® 488. Short hairpin RNA transfections were done 48 h before performing the assays, using the pSicoR vector, carrying a green fluorescent protein expression cassette and containing the short hairpin RNA sequence of choice. Targeting sequences for Fgd4: 5′-GCA GCA AGC CAT TCT AAT-3′ (shRNA1) and 5′-GAA GAA GAG GAT ATT GTA-3′ (shRNA2). Control short hairpin RNA (targeting dsred2): 5′-AGT TCC AGT ACG GCT CCA A-3′ (Ozcelik *et al.*, 2010).

Transferrin assays

Transferrin assay for fluorescence-activated flow cytometry was performed as described (Sidiropoulos *et al.*, 2012) using short hairpin or small interfering RNA-transfected RT4 cells. Fluorescence intensity of internalized transferrin was measured for 2000 green fluorescent protein- (short hairpin RNA transfections) or Alexa Fluor® 488-positive (small interfering RNA transfections) cells. High expressing cells were subjected to comparative analysis. For fluorescence microscopy, the identical assay was performed with the exceptions that Alexa Fluor® 555-labelled transferrin (Invitrogen; 20 μg/ml in serum-free Dulbecco's modified Eagle's medium) was used and cells were not detached before fixation. Images were captured with an epifluorescence Zeiss Axiovert microscope equipped with a Zeiss High Resolution Monochromatic camera.

Western blotting and antibodies

Sciatic nerves from adult mice were isolated and separated from the epineurium. Nerves were homogenized with a chilled mortar and pestle in lysis buffer (0.1% SDS, 10 mM Tris–HCl, 150 mM NaCl, 50 mM NaF, 1 mM $NaVO_4$, 1 mM EDTA, 0.5% sodium-deoxycholate, protease inhibitor mixture; Sigma). Extracts were processed using standard SDS-PAGE and western blotting procedures. The following antibodies were used: AKT-P Serine 473 (Cell Signaling Technology, 1:1000), AKT (Cell Signaling Technology, 1:1000), ErbB2-P Tyrosine 1248 (Abcam, 1:1000), ErbB2 (Abcam, 1:1000), disc large homologue 1 (Dlg1) (BD Transduction Laboratories, 1:1000), myelin basic protein (AbD Serotec, 1:1000), JNK-P Threonine 183/Tyrosine 185 (c-jun-N-terminal kinase) (Cell Signaling, 1:1000), JNK (Cell Signaling, 1:1000), Cdc42 (Abcam, 1:1000 and Cell Signaling, 1:1000), Frabin/Fgd4 (Pineda, 1:1000; peptide used for rabbit immunization: SKGKHSKVSDLISHFE), Frabin/Fgd4 (Transduction Laboratories, 1:500), α-tubulin (Sigma, 1:1000) and glyceraldehyde-3-phosphate dehydrogenase (HyTest, 1:10 000). Secondary antibodies were obtained from Promega and Southern Biotech. Bands were quantified using Quantity One® software (Bio-Rad).

Cryo-embedding and immunostaining of cryosections

Sciatic nerves were removed from mice, fixed in 4% paraformaldehyde for 1 h, incubated overnight in 30% sucrose and frozen in OCT (Tissue Tek). Sections (10 μm) were cut on a HM560 Cryostat (Microm), post-fixed in 4% paraformaldehyde for 5 min, blocked in blocking solution (10% goat serum in PBS with 0.3% Triton® X-100) for 1 h at room temperature and incubated with primary antibodies against S100β (Sigma, mouse monoclonal, 1:200) and Frabin/Fgd4 (Pineda, rabbit polyclonal, 1:200) overnight at 4°C in blocking solution. Sections were washed with PBS and incubated with secondary antibodies against mouse coupled to Alexa Fluor® 488 (Invitrogen, 1:500) and rabbit coupled to Cy3 (Jackson ImmunoResearch, 1:500) for 1 h at room temperature. Sections were washed with PBS, incubated for 5 min with 4′,6-diamidino-2-phenylindole and mounted with Immu-Mount™ (Thermo Scientific).

Statistical analysis

Data show the mean ± standard error of the mean. Two-tailed Student's *t*-test was used with significance set to $*P < 0.05$, $**P < 0.01$ or $***P < 0.001$; *n* = number of independent experiments.

Results

Ubiquitous loss of Frabin/*Fgd4* induces features of a demyelinating peripheral neuropathy in mice

We have generated a conditional mouse null allele for Frabin/*Fgd4* using standard embryonic stem cell technology. To achieve this goal, exon 4 of *Fgd4* was flanked with LoxP sites by homologous recombination, and mice with this allele were obtained (Fig. 1A).

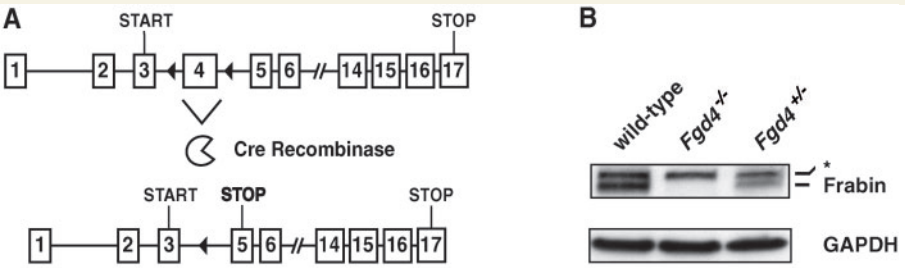

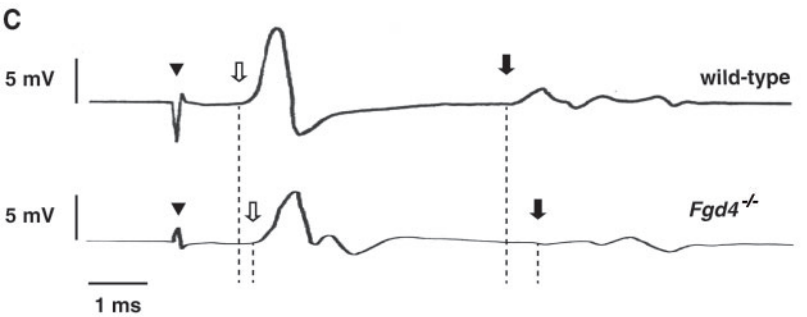

D

	wild-type	*Fgd4*$^{-/-}$	*P*
Distal latency (ms)	0.82 (± 0.02)	1.09 (± 0.04)	***
CMAP amplitude (mV)	11.7 (± 1.18)	7.91 (± 1.07)	*
NCV (m/s)	48.0 (± 3.83)	38.7 (± 1.00)	*
F-wave latency (ms)	4.43 (± 0.09)	4.86 (± 0.05)	***

Figure 1 Loss of Frabin/Fgd4 leads to electrophysiological characteristics of demyelinating peripheral neuropathies. (**A**) Ablation of exon 4 in the *Fgd4* locus generates a premature stop codon in exon 5 because of a frame shift (filled triangles = introduced loxP sites; START = translational start codon; STOP = conventional translational stop codon; STOP (bold) = premature translational stop codon generated after *Fgd4* exon 4 ablation), resulting in **B**, loss of Frabin/Fgd4 protein (western blot; asterisk: unspecific signal). (**C** and **D**) At 60 weeks, *Fgd4*$^{-/-}$ mice show longer distal latency, disperse compound muscle action potentials with mild reduction in amplitude, longer F-wave latency and reduced nerve conduction velocity in sciatic nerve compared with wild-type mice; in **C**, a representative original recording is shown. Arrowhead indicates stimulus artefact; open arrow indicates onset of compound muscle action potential (distal latency); filled arrow indicates onset of F-wave. Data represent the mean ± standard error of the mean. Wild-type mice, *n* = 7; *Fgd4*$^{-/-}$ mice, *n* = 10. *P*-values in **D**: $*P < 0.05$; $***P < 0.001$; Student's *t*-test (two-tailed).

In our initial experiments, we bred and analysed a mouse line that lacks Frabin/Fgd4 ubiquitously. This approach mimics the genetic situation in patients with CMT4H and was aimed to assess whether FRABIN/*FGD4* mutations are definitively responsible for CMT4H, and mice lacking Frabin/Fgd4 constitute an appropriate animal model for this disease. In addition, we anticipated that Frabin/Fgd4-deficient mice would be suitable to study Frabin/Fgd4 function *in vivo*. For this purpose, we bred mice carrying conditional *Fgd4* alleles (*Fgd4* flox) with mice expressing Cre recombinase in the germline. This procedure resulted in offspring with a constitutively inactivated *Fgd4* allele. As expected, mice homozygous for this deletion allele ($Fgd4^{-/-}$) are lacking Frabin/Fgd4 protein expression as verified by western blot analysis of sciatic nerve lysates (Fig. 1B). $Fgd4^{-/-}$ mice are viable, fertile and were born at expected Mendelian ratios. We found no major abnormal behaviour by SHIRPA (SmithKline Beecham, Harwell, Imperial College, Royal London Hospital, phenotype assessment) analysis up to the age of 60 weeks. Frabin/Fgd4 mutants displayed normal body size and weight and were inconspicuous in sensory examinations (Supplementary Table S1). In a grip strength test, 60-week-old $Fgd4^{-/-}$ mice exhibited mildly impaired performance compared with wild-type mice. However, we found no significant differences in rotarod performance and footprint analysis (step length, step width and foot angle), collectively indicating a mild phenotype at this age.

As CMT4H belongs to the demyelinating forms of peripheral neuropathies, we expected characteristic electrophysiological alterations in myelinated nerves of $Fgd4^{-/-}$ mice. Indeed, when analysing the function of motor fibres, we detected moderately increased distal latencies and mildly increased F-wave latencies, reduced nerve conduction velocity and dispersed compound muscle action potentials with mildly reduced amplitudes in 60-week-old $Fgd4^{-/-}$mice compared with wild-type mice (Fig. 1C and D), whereas at 30 weeks of age no abnormalities were observed (data not shown).

These electrophysiological alterations are consistent with a demyelinating phenotype caused by loss of Frabin/Fgd4. To corroborate the findings, we performed histological examinations of distal peripheral nerves with variable motor and sensory contributions (plantaris, sciatic, quadriceps and saphenous) and of proximal parts of motor and sensory nerves [lumbar spine nerve roots 4 (L4) ventral and dorsal roots]. An overview revealed aberrant myelin structures in all analysed nerves of $Fgd4^{-/-}$ mice, albeit with different frequencies (Fig. 2 and Supplementary Fig. 1). The predominant irregular features were myelin outfoldings and infoldings of various complexities, in combination with redundant myelin loops, both around nodes of Ranvier and along internodes. In addition, we found axons in older animals without myelin or with abnormally thin myelin, indicating demyelination and incomplete remyelination. Myelin debris and polyaxonal myelination were occasionally observed.

Based on this survey, we performed quantitative temporal examinations in developing and adult mice. Our initial qualitative investigations in the sciatic nerve provided evidence that aberrant myelin features might already be increased in early $Fgd4^{-/-}$ nerve development compared with wild-type mice (Fig. 2A–D). Thus, we analysed and quantified, at the ultrastructural level by electron microscopy, the number of fibres that displayed aberrant myelin structures on complete reconstructions of post-natal Day 5 sciatic nerves. A subtle, but significant surplus of affected fibres was found in $Fgd4^{-/-}$ mice compared with wild-type mice (Fig. 3), confirming an early onset of this characteristic morphological phenotype. To examine phenotype progression over time, we tracked alterations in the plantaris nerve, as this distal nerve is a sensitive indicator of nerve changes in mouse models of hereditary motor and sensory neuropathies (Frei *et al.*, 1999; our unpublished observations). $Fgd4^{-/-}$ mice displayed significantly more fibres with aberrant myelin structures compared with wild-type mice at all time points analysed from post-natal Day 14 to 80 weeks of age (Fig. 4A and B). These alterations became progressively more severe with ~6% of affected fibres at 2 weeks of age and reaching 40% in 80-week-old $Fgd4^{-/-}$ mice. In parallel, the complexity and extent of aberrant myelin structures associated with individual axons increased with age as judged by qualitative examinations (Fig. 4A). Myelinated axons without overt myelin aberrations had normal myelin thickness as assessed by growth ratio (axon diameter/fibre diameter) measurements in 10-week-old animals (Fig. 4C). In 60-week-old animals, however, we observed a tendency towards an increased growth ratio, indicating thinner myelin (Fig. 4D). In line with these findings, the number of fibres with signs of demyelination and partial remyelination revealed a tendency towards an increase in 60-week-old $Fgd4^{-/-}$ mice compared with wild-type mice, reaching statistical significance in 80-week-old animals (Fig. 4E). Remarkably, we found a rather steep rise in demyelination/remyelination features between 60- and 80-week-old $Fgd4^{-/-}$ animals, suggesting that demyelination proceeds rapidly when a threshold of damage is reached. On the axonal side, quantification of myelinated axons of entire plantaris nerves revealed no significant difference between $Fgd4^{-/-}$ and wild-type mice at all ages examined up to 80 weeks, indicating no major primary or secondary axonal loss (Fig. 4F). In summary, our findings show that loss of Frabin/Fgd4 in the mouse leads to electrophysiological and morphological abnormalities resembling the hallmarks of CMT4H, thus establishing $Fgd4^{-/-}$ mice as an animal model for this disorder.

Schwann cells critically depend on Frabin/Fgd4 function

Intimate and reciprocal Schwann cell–axon interactions are a major regulatory hallmark of peripheral nerves in health and disease (Suter and Scherer, 2003; Jessen and Mirsky, 2005; Nave and Trapp, 2008; Salzer, 2008; Taveggia *et al.*, 2010; Pereira *et al.*, 2012). Thus, our findings in $Fgd4^{-/-}$ mice may be because of a primary requirement of Frabin/Fgd4 function in either Schwann cells or neurons, or both the cell types. The answer to this question is important to understand why and how peripheral nerves rely on Frabin/Fgd4, and this knowledge will provide critical insights into the CMT4H disease mechanism. Thus, we bred mice carrying the conditional Frabin/*Fgd4* null allele (Fig. 1A) with established mouse lines that express Cre recombinase specifically in the Schwann cell lineage Dhh-Cre (Jaegle *et al.*, 2003; Pereira *et al.*, 2009) or in the motor neuron lineage (Hb9-Cre; Arber

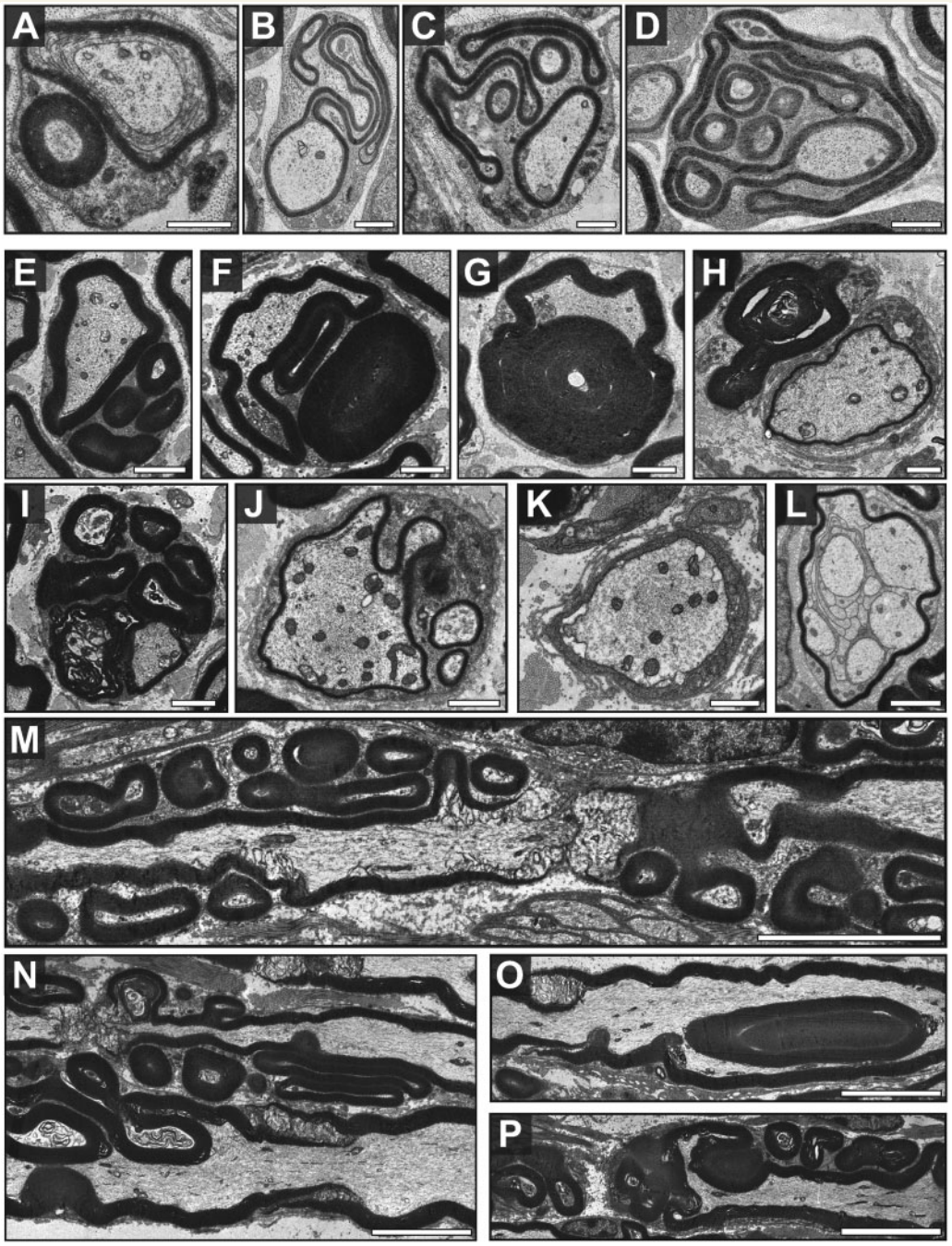

Figure 2 Frabin/Fgd4-deficient mice form aberrant PNS myelin. *Fgd4*$^{-/-}$ mice display aberrant myelin features during early steps of myelination (**A–D**: post-natal Day 5; sciatic nerve) and in myelin maintenance (**E–G**, **I** and **K**: 80 weeks old mice; **H**, **J** and **M–P**: 60 weeks old mice; **L**: 10 weeks old mice; plantaris nerve), including simple myelin outfoldings (**A**), redundant myelin (**B**), complex myelin outfoldings (**E**) and highly complex myelin outfoldings (**C** and **D**), redundant myelin loops outside (**F**) and protruding into the axon (**G**), degradation of myelin (**I**), signs of demyelination (**K**) and remyelination (**H** and **J**) and rarely polyaxonal myelination (**L**). Aberrant myelin features tend to be located in the vicinity of nodes of Ranvier and Schmidt–Lanterman incisures (**M**, **N** and **P**). (**A–L**) Cross-sections. (**M–P**) Longitudinal sections. Scale bars = 1 μm (**A–L**); 5 μm (**M–P**).

et al., 1999) (Fig. 5A). Dhh-Cre *Fgd4* flox/flox animals (Dhh-Cre; Fig. 5B) and Hb9-Cre *Fgd4* flox/flox animals (Hb9-Cre; Fig. 5C) displayed loss of Frabin/Fgd4 in the targeted cell type as expected. Qualitative histological analysis of various adult peripheral nerves revealed prominent aberrant myelin features in conditional *Fgd4* mutants with Schwann cell-specific Frabin/Fgd4 deletion, comparable with those observed in *Fgd4*$^{-/-}$ mice (Fig. 5D). In contrast, nerves of motor neuron-specific Frabin/Fgd4 deletion mutants were not different from the wild-type mice. For quantitative analysis, we examined fully reconstructed sections of

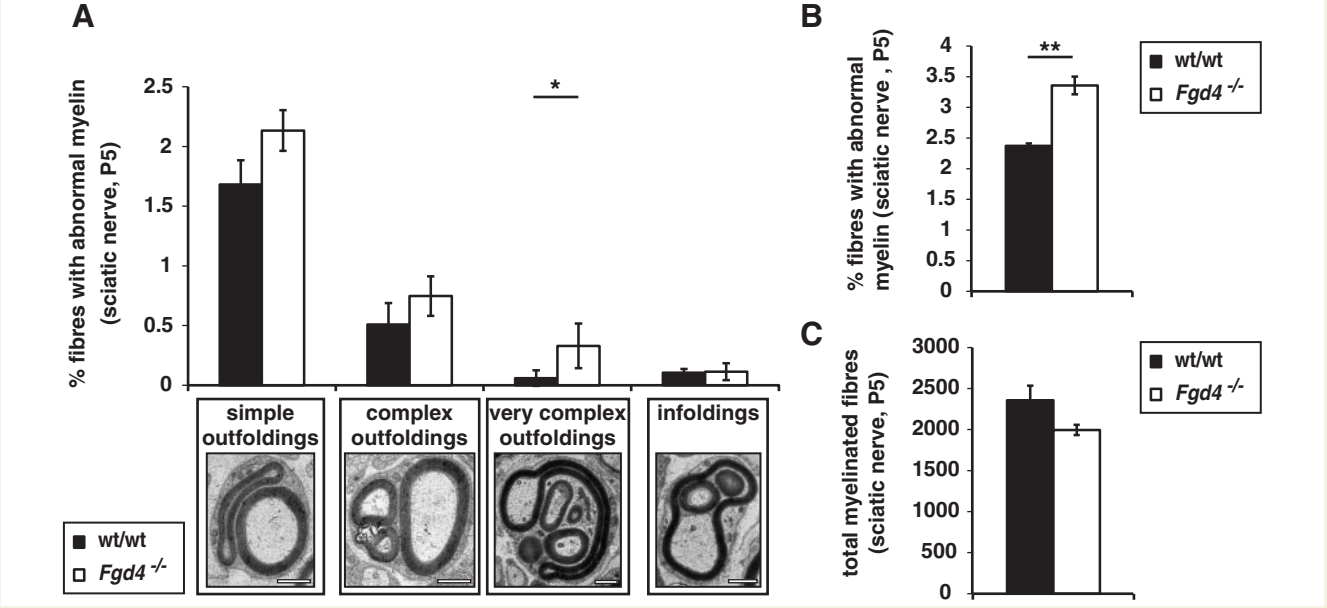

Figure 3 Aberrant development of PNS myelination in *Fgd4*$^{-/-}$ mice. (**A**) Aberrant myelin structures of post-natal Day 5 (P5) sciatic nerves were categorized in four sets (simple, complex, very complex outfoldings and infoldings) and quantified at electron microscopy level. Very complex outfoldings were significantly increased in *Fgd4*$^{-/-}$ animals. (**B**) Overall number of fibres showing aberrant myelin features was also increased in Frabin/Fgd4-deficient mice. (**C**) Total number of myelinated fibres was not significantly altered between *Fgd4*$^{-/-}$ and wild-type (wt/wt) animals. Three mice per genotype were analysed. Scale bars = 1 μm. *$P < 0.05$, **$P < 0.01$ Student's *t*-test (two-tailed).

plantaris- (60-week-old), quadriceps- and saphenous nerves (30 weeks old), derived from mice with Schwann cell-specific or motor neuron-specific Frabin/Fgd4 deletions, in a comparative analysis with age-matched nerves of *Fgd4*$^{-/-}$ animals at the electron microscopy level. Strikingly, these studies showed that in all three nerves, Schwann cell-specific Frabin/Fgd4 loss generated a morphological phenotype (aberrant myelin structures) quantitatively indistinguishable from *Fgd4*$^{-/-}$ animals (Fig. 5E). Overall numbers of myelinated fibres showed no relevant alterations in all examined nerves and genotypes. Taken together, our findings demonstrate that loss of Frabin/Fgd4 function in Schwann cells is primarily responsible for the observed myelin aberrations in adult *Fgd4*$^{-/-}$ mice without detectable contributions from motor neurons.

Frabin/*Fgd4* function in Schwann cells is required for myelin maintenance

The availability of a conditional Frabin/*Fgd4* null allele allowed us to also address the physiologically and pathophysiologically important issue whether Frabin/Fgd4 is required for the maintenance of properly developed myelin, independent from the role of Frabin/Fgd4 in myelination during development. To answer this question, we bred mice carrying the conditional Frabin/*Fgd4* null allele with an established Plp-CreERT2 mouse line (Leone *et al.*, 2003). In the offspring, Cre-mediated recombination in Schwann cells was induced by tamoxifen injections in young adult Plp-CreERT2 *Fgd4* flox/flox animals (10 weeks old) (Fig. 6A). Specific loss of Frabin/Fgd4 in Schwann cells was verified by immunostaining (Fig. 6B). Qualitative analysis of plantaris nerves derived from such adult-induced Frabin/Fgd4 mutants at the age of 30 weeks revealed aberrant myelin features similar to age-matched *Fgd4*$^{-/-}$ animals (Fig. 6C). Quantifications of whole-nerve reconstructions at the electron microscopy level showed that adult-induced Frabin/Fgd4 mutants had slightly fewer affected plantaris nerve fibres compared with *Fgd4*$^{-/-}$ mice (~10 versus 15%). However, there was still a strong increase in myelin alterations in adult-induced Frabin/Fgd4 mutants compared with wild-type or tamoxifen-injected control mice (~10 versus 2%; Fig. 6D). These data demonstrate a critical function of Frabin/Fgd4 in myelin maintenance and imply that the observed phenotype in *Fgd4*$^{-/-}$ mice reflects both a developmental and a maintenance component.

Frabin/*Fgd4* controls Cdc42 activity in peripheral nerves

Next, we addressed whether loss of Frabin/Fgd4 alters signalling pathways known to be critical in peripheral nerve myelination (Pereira *et al.*, 2012). In particular, alterations in neuregulin signalling and the AKT pathway have been associated with hypermyelination, myelin outfoldings and demyelination (Cotter *et al.*, 2010; Goebbels *et al.*, 2010, 2012). However, we found no significant differences of total and active levels of AKT and ErbB2 and of the amounts of the regulatory phosphatase and tensin homologue (PTEN)-interactor Dlg1 in sciatic nerve lysates derived from 10-week-old *Fgd4*$^{-/-}$ mice compared with wild-type mice by western blot analysis (Fig. 7A and B). JNK levels and JNK

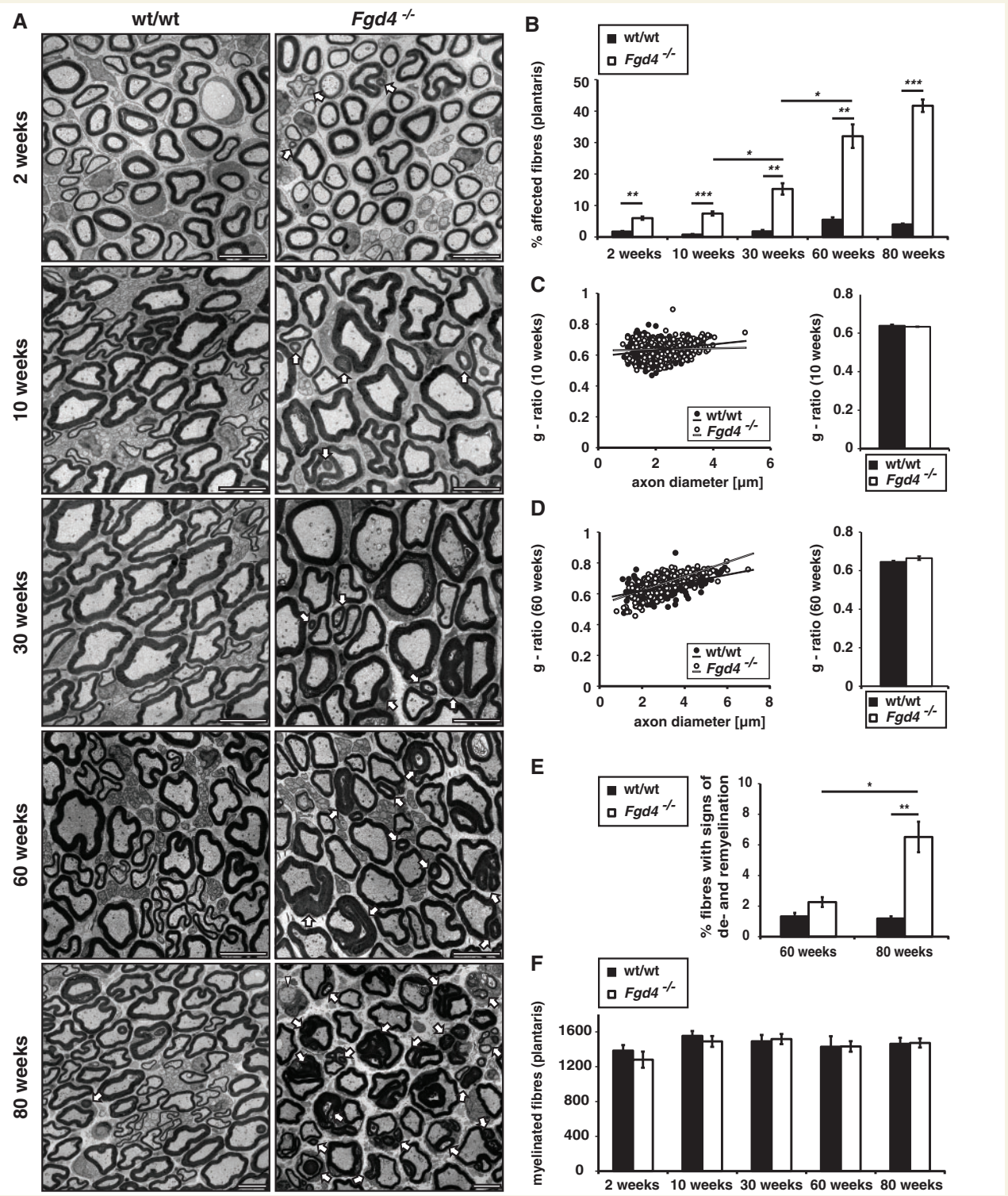

Figure 4 *Fgd4*$^{-/-}$ mice develop a progressive demyelinating neuropathy with aberrant myelin formation. (**A**) Transverse sections of plantaris nerves show a temporally progressive accumulation of aberrant myelin features in *Fgd4*$^{-/-}$ mice compared with wild-type (wt/wt) mice aged 2–80 weeks. (**B**) Quantification of aberrant myelin features on entire transversal nerve reconstructions at electron microscopy level reveals a significant and progressive increase in the amount of affected fibres in *Fgd4*$^{-/-}$ mice aged 2–80 weeks. (**C** and **D**) G-ratio is not significantly changed between wild-type and *Fgd4*$^{-/-}$ mice aged 10 and 60 weeks (at least 100 fibres quantified per animal). (**E**) Signs of demyelination and remyelination accumulate significantly between the age of 60 and 80 weeks in *Fgd4*$^{-/-}$ mice, the difference to wild-type (wt/wt) mice reaching significance by 80 weeks. (**F**) No loss in the overall number of myelinated fibres was detectable up to the age of 80 weeks. Arrows indicate fibres displaying myelin alterations. Arrowhead indicates demyelinated fibre. Scale bars = 5 µm; $*P < 0.05$, $**P < 0.01$, $***P < 0.001$; Student's *t*-test (two-tailed). Three animals were analysed for each genotype per time point.

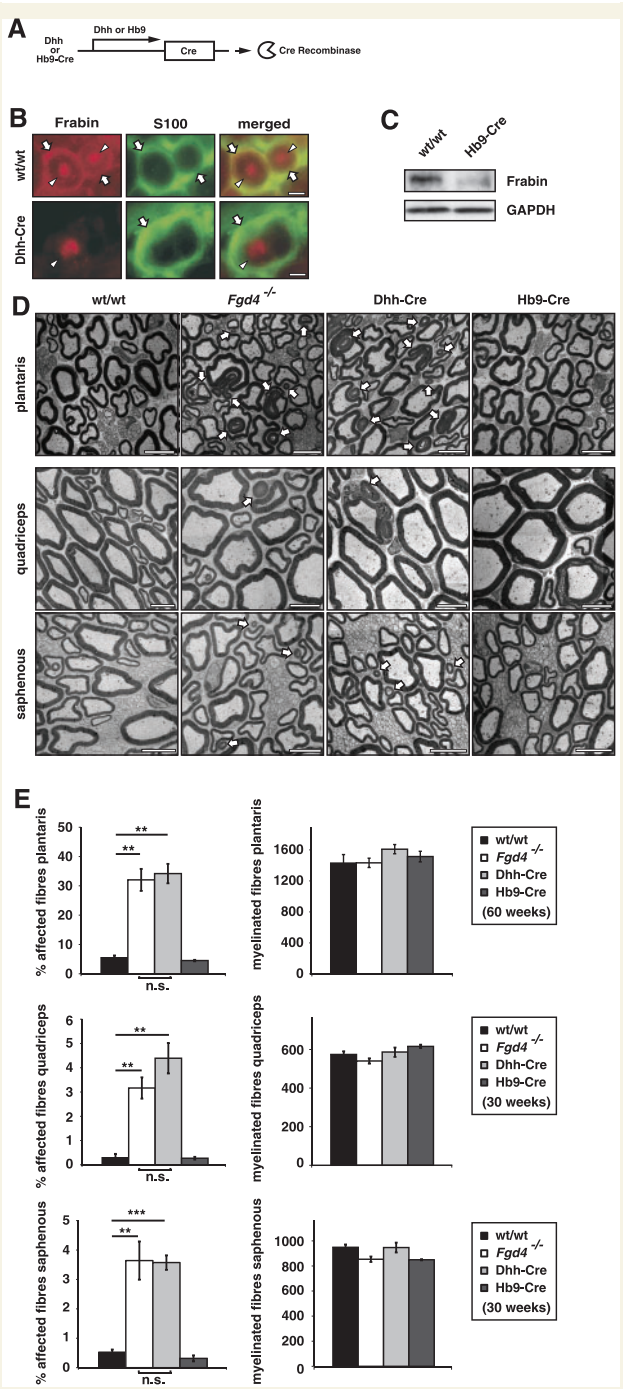

Figure 5 Cell type-specific gene ablation reveals that Schwann cells require Frabin/Fgd4 for proper myelination. (**A**) Schwann cell- or motor neuron-specific ablation of *Fgd4* by Dhh- or Hb9-gene regulatory elements-driven Cre recombinase (Dhh- or Hb9-Cre/*Fgd4* flox/flox animals) results in **B**, Schwann cell-specific (Dhh-Cre) loss of detectable Frabin/Fgd4 on cryosections of sciatic nerves (white arrows mark Schwann cells, arrowheads mark axons) or (**C**) strongly reduced Frabin/Fgd4 expressed by motor neurons (Hb9-Cre) as shown by western blot analysis of mutant ventral roots lysates compared with wild-type (wt/wt). (**D**) Schwann cell-specific loss of Frabin/Fgd4 (Dhh-Cre) in plantaris nerves of 60-week-old mice or quadriceps and saphenous nerve of 30-week-old mice leads to aberrant myelin formation, similar to that seen in $Fgd4^{-/-}$ mice (white arrows mark aberrant myelin features). Motor neuron-specific ablation of Frabin/Fgd4 (Hb9-Cre), however, does not result in a detectable pathological phenotype at electron microscopy level in plantaris, quadriceps or saphenous nerves at the corresponding ages. (**E**) Quantification of aberrant myelin features shown in **D**. Note the similar numbers of fibres with aberrant myelin features (affected fibres) present in DhhCre/*Fgd4* flox/flox mice (Dhh-Cre) compared with $Fgd4^{-/-}$ mice. Both are significantly increased compared with wild-type mice (wt/wt). The numbers in Hb9Cre/*Fgd4* flox/flox mice (Hb9-Cre), however, were not different from wild-type mice. Total numbers of myelinated fibres were not changed in all genotypes. Three mice were analysed for each genotype, time point and type of nerve. Scale bars = 5 μm; n.s. = not significant. $*P > 0.05$, $**P < 0.01$, $***P < 0.001$; Student's *t*-test (two-tailed). GADPH = glyceraldehyde-3-phosphate dehydrogenase.

phosphorylation were also not altered. In addition, the amount of myelin basic protein that we examined as a representative myelin protein was unchanged.

On the molecular level, Frabin/Fgd4 has been reported to act as a Cdc42-specific GEF (Umikawa *et al.*, 1999), and loss of Cdc42 in Schwann cells is incompatible with proper developmental myelination (Benninger *et al.*, 2007). Thus, we analysed Cdc42 and found that its active form Cdc42-GTP was substantially and significantly reduced in sciatic nerves of adult $Fgd4^{-/-}$ mice compared with age-matched wild-type mice (Fig. 7C and D). As total levels of Cdc42 remained unchanged, the ratios of active-Cdc42/total-Cdc42 and active-Cdc42/glyceraldehyde-3-phosphate dehydrogenase (as an indirect measure of active Cdc42 per cellular unit) were also reduced. These findings support the hypothesis that Frabin/Fgd4 acts as a GEF for Cdc42 in peripheral nerves *in vivo*, as RhoGEFs shift the equilibrium between active and total amounts of RhoGTPases towards the active forms (Etienne-Manneville and Hall, 2002).

Cdc42 is required for peripheral nerve myelin maintenance

Our data indicated that Frabin/Fgd4 in Schwann cells is essential for maintenance of proper myelin, and the activation of Cdc42 in $Fgd4^{-/-}$ nerves is strongly decreased. Based on these findings, we hypothesized that if the critical function of Frabin/Fgd4 in myelin maintenance involves correct Cdc42 activation, Schwann cell-specific elimination of Cdc42 at adult stages should also cause myelin deficiencies. To address this question, we combined mice carrying floxed Cdc42 alleles, which were previously used to analyse the role of Cdc42 in Schwann cell development (Benninger *et al.*, 2007), with mice carrying the Plp-CreERT2 transgenic allele. The experimental setting used was analogous to that described earlier for Frabin/Fgd4 deletion in adult myelinating Schwann cells (Fig. 8A). Cdc42 deletion was induced in 10-week-old animals, and western blot analysis revealed subsequent loss of Cdc42 as expected (Fig. 8B). Thereafter, we analysed sciatic nerves of 10-month-old animals by standard electron microscopy and FIB-SEM (serial electron microscopy coupled with *in situ* focused ion beam milling; Pereira *et al.*, 2010). Prominent myelin foldings were present in nerves with adult-onset Cdc42 deletion (Fig. 8C

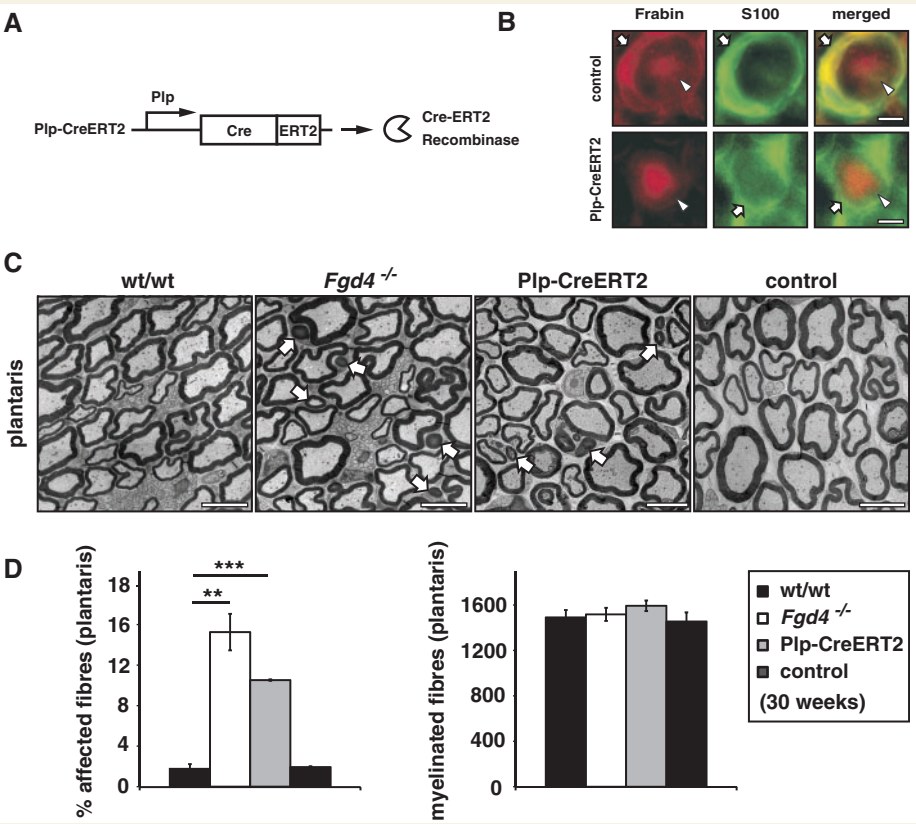

Figure 6 Inducible Schwann cell-specific gene ablation reveals that myelin maintenance depends on Frabin/Fgd4. (**A**) Tamoxifen-mediated induction of Frabin/Fgd4 ablation in 10-week-old *Fgd4* flox/flox mice through activation of Plp promotor-driven Cre recombinase (Plp-CreERT2) results in (**B**) Schwann cell-specific loss of Frabin/Fgd4 protein in peripheral nerves of adult mice, shown on cryosections of sciatic nerve, 4 months after tamoxifen injections (arrow: Schwann cell; arrowhead: axon). (**C**) Aberrant myelin formation in plantaris nerves of 30-week-old Plp-CreERT2/*Fgd4* flox/flox (Plp-CreERT2) mice, tamoxifen-treated at 10 weeks of age as control mice, compared with age-matched $Fgd4^{-/-}$ and wild-type (wt/wt) mice. (**D**) Quantification of myelinated fibres displaying aberrant myelin features (affected fibres) of identically obtained nerves as shown in **C**, revealing significantly increased numbers of affected fibres in Plp-CreERT2/*Fgd4* flox/flox mice (Plp-CreERT2) compared with wild-type or tamoxifen-injected control mice. Comparison of Plp-CreERT2 with $Fgd4^{-/-}$ mice shows only a slight reduction in affected fibres. Total numbers of myelinated fibres were unchanged between the groups. Three mice were analysed for each group in all experiments. Scale bars = 5 μm. White arrows indicate affected fibres. $^{**}P < 0.01$, $^{***}P < 0.001$; Student's *t*-test (two-tailed).

and D; Supplementary Videos 1 and 2) comparable with our previous findings with adult-onset Frabin/Fgd4 deletions (Fig. 6).

Frabin/Fgd4 regulates endocytosis in Schwann cells

We then asked which cellular functions of Schwann cells might be critically dependent on Frabin/Fgd4. Thus, we analysed migration and process extensions of cultured rat Schwann cells after efficient short hairpin RNA-mediated Frabin/Fgd4 expression knock-down. However, both processes were not altered compared with control cells (data not shown). As myelination depends strongly on endocytosis (Stendel *et al.*, 2010; Sidiropoulos *et al.*, 2012), we also tested whether Frabin/Fgd4 regulates this crucial cellular process. First, we examined whether knock-down of Frabin/Fgd4 affects Cdc42 in cultured Schwann cells. Indeed, reduced Frabin/Fgd4 levels led to lower amounts of active Cdc42 in the rat schwannoma cell line RT4 (Fig. 9A and B), consistent with our *in vivo* data (Fig. 7C). Next, we examined endocytosis efficiency with an established transferrin uptake assay in Frabin/Fgd4-silenced RT4 cells (Sidiropoulos *et al.*, 2012). Reduced transferrin uptake was found in such cells with ~20% decrease compared with control cells (Fig. 9C and D). We conclude that regulation of Schwann cell endocytosis by Frabin/Fgd4 is likely to contribute to the disease mechanism in CMT4H.

Discussion

Frabin-deficient mice as an animal model for CMT4H

During the past 15 years, transgenic animal models for inherited peripheral neuropathies have become essential tools for dissecting

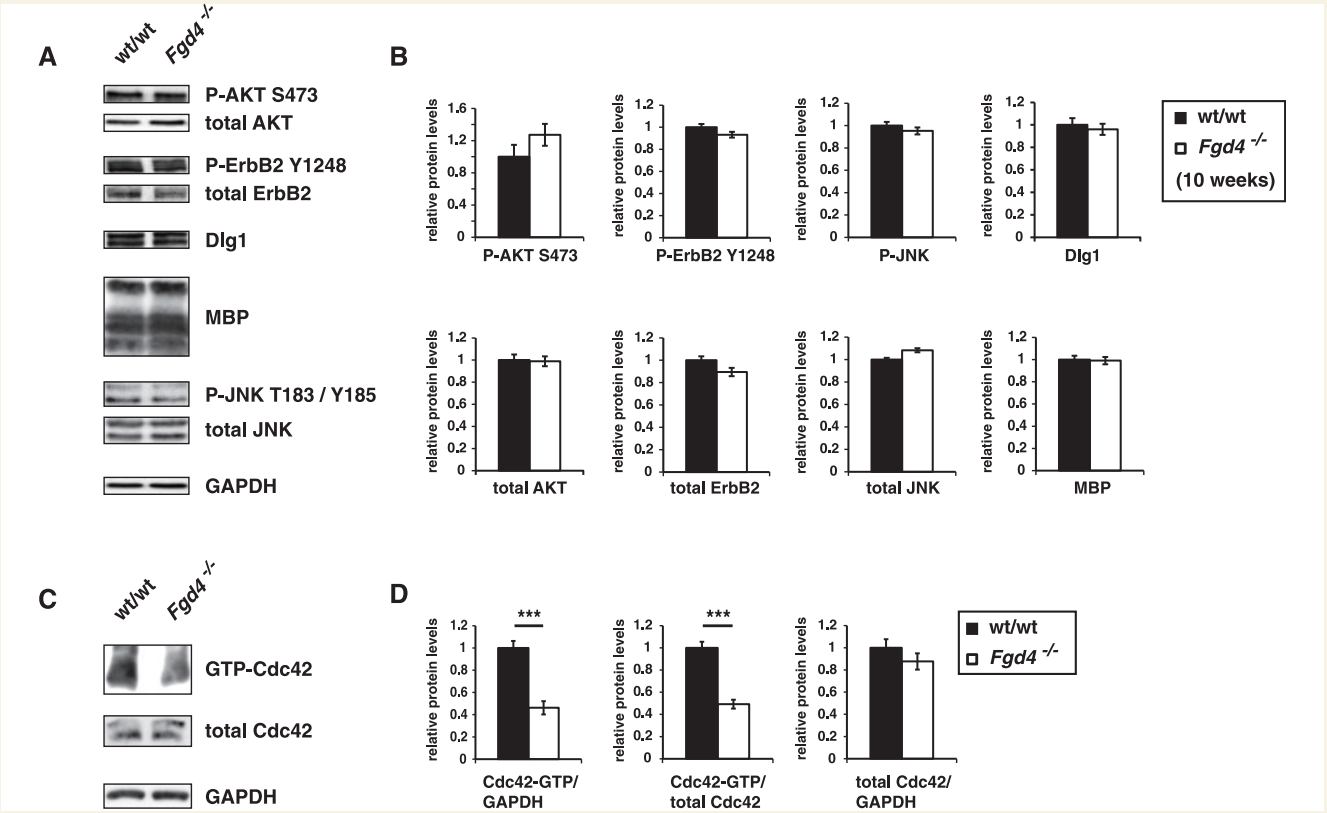

Figure 7 Ablation of Frabin/Fgd4 reduces activation of the RhoGTPase Cdc42 in peripheral nerves *in vivo*. (**A** and **B**) Western blot analyses demonstrating that total and active levels of AKT, ErbB2 receptor and JNK, and total levels of MBP and Dlg1, are not changed in sciatic nerve of $Fgd4^{-/-}$ mice compared with wild-type (wt/wt) mice at the age of 10 weeks. (**C** and **D**) Active, but not total levels of Cdc42 are significantly reduced in sciatic nerves of adult $Fgd4^{-/-}$ mice compared with age-matched wild-type mice. Tissues from four wild-type and $Fgd4^{-/-}$ mice were analysed. ***$P < 0.001$; Student's *t*-test (two-tailed). GADPH = glyceraldehyde-3-phosphate dehydrogenase.

pathological mechanisms involved in various subtypes of Charcot–Marie–Tooth disease (Suter and Nave, 1999; Nave *et al.*, 2007). Such models also provided the basis for evaluating treatment strategies (Fledrich *et al.*, 2012*a*, *b*) and contributed significantly to our current understanding of the molecular mechanisms that govern myelination (Pereira *et al.*, 2012). With the $Fgd4^{-/-}$ mouse line, we present the generation and analysis of an animal model for CMT4H because of loss of Frabin/Fgd4. As in CMT4H patients, $Fgd4^{-/-}$ mice are affected by a recessive, dysmyelinating and demyelinating peripheral neuropathy with early onset and progressive course upon histological examination. Mouse nerves revealed myelin infoldings and outfoldings, redundant myelin loops and signs of demyelination and remyelination, analogous to neuropathological features seen in CMT4H biopsies. Taking advantage of the fact that animal models allow detailed spatial and temporal analyses, we found that both sensory and motor fibres are similarly affected if Frabin/Fgd4 is missing. Moreover, nerve fibres were distally strikingly more affected than proximally, in line with the distally accentuated neuropathy in CMT4H. The reasons for this rather generally observed phenomenon in Charcot–Marie–Tooth disease pose a persisting question, still lacking completely satisfactory answers. Potential explanations include higher susceptibility to mechanical stress of distal fibre segments or transport impairments along the axons that are reflected in this manner. Of major conceptual importance, temporal quantitative analysis of pathological features revealed significant myelin alterations already at early stages of myelination (post-natal Day 5), continuously increasing with age. Thus, loss of Frabin/Fgd4 harms nerves early in development suggesting that early-onset dysmyelination contributes to CMT4H. Furthermore, the observed increase in pathological features with age is consistent with the slowly progressive course of CMT4H. Interestingly, we found the classical hallmarks of demyelinating Charcot–Marie–Tooth disease, demyelination and remyelination associated with reduced nerve conduction velocity, only in older animals. In addition, these features were generally milder than in patients with CMT4H, in agreement with other mouse models for demyelinating Charcot–Marie–Tooth disease showing milder neurological pathology than the corresponding patients (Martini, 2000). This discrepancy is particularly striking when Myotubularin-related protein-2 or Myotubularin-related protein-13/Set-binding factor-2-deficient mice and their human counterparts, the autosomal recessive Charcot–Marie–Tooth disease subtypes CMT4B1 or CMT4B2, are compared (Bolino *et al.*, 2000; Azzedine *et al.*, 2003; Senderek *et al.*, 2003; Bolino *et al.*, 2004; Bonneick *et al.*, 2005; Tersar *et al.*, 2007; Robinson *et al.*, 2008). Incidentally, the neuropathological

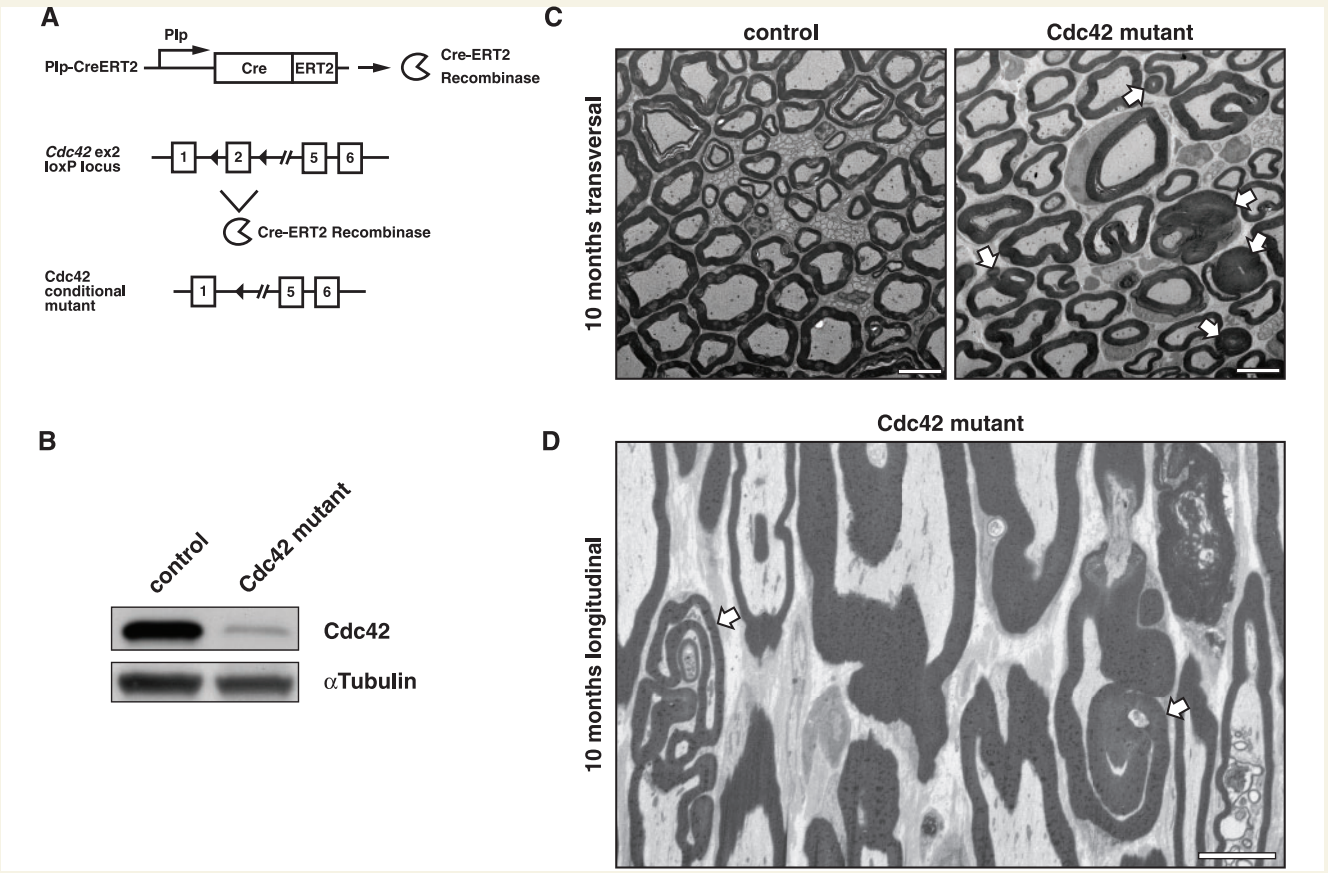

Figure 8 Inducible gene ablation reveals that loss of Cdc42 in adult myelinating Schwann cells causes histopathological aberrations phenocopying loss of Frabin/Fgd4. (**A**) Tamoxifen-mediated induction of Cdc42 ablation in 10-week-old *Cdc42* flox/flox mice through activation of Plp promotor-driven Cre recombinase (Plp-CreERT2) results in (**B**) strongly reduced Cdc42 protein as shown by western blot analysis of sciatic nerve lysates obtained 7 months post-tamoxifen injection. (**C**) Aberrant myelin formations, including outfoldings and redundant myelin, in sciatic nerves of 10 months old PlpCreERT2/*Cdc42* flox/flox (Cdc42 mutant) mice (electron microscopy cross-sections). (**D**) Representative FIB-SEM-derived longitudinal section of Cdc42 mutant sciatic nerves prepared as in **C** (see also Supplementary Videos 1 and 2) showing myelin outfoldings in the vicinity of nodes of Ranvier. Scale bars = 5 μm. White arrows indicate fibres with aberrant myelin features.

features in these mutants with regards to the observed myelin abnormalities are virtually identical compared with Frabin/Fgd4 mutants.

Loss of Frabin/Fgd4 function in Schwann cells is sufficient to induce a CMT4H-like phenotype

Demyelinating Charcot–Marie–Tooth disease neuropathies are usually attributed to an initial Schwann cell-specific damage, as myelin constitutes a Schwann cell compartment. However, the possibility of axonal contributions cannot be excluded, as establishment and maintenance of the myelin sheath depend on axonal signals and continuous bidirectional Schwann cell–axon communication (Pereira *et al.*, 2012). We found that Frabin/Fgd4 is expressed in mouse Schwann cells and PNS neurons, compatible with a functional role of Frabin/Fgd4 in both cell types. Thus, we dissected the cell type-specific implications of Frabin/Fgd4 loss by genetically ablating Frabin/Fgd4 exclusively either in Schwann cells or in motor neurons. This experimental strategy also allowed us to determine which cell type is primarily dependent on Frabin/Fgd4 function in myelination. Schwann cell-specific ablation of Frabin/Fgd4 alone was sufficient to fully replicate the myelin aberrations observed in *Fgd4*$^{-/-}$ mice. In contrast, we found no differences in motor neuron-specific Frabin/Fgd4-deficient mice compared with wild-type mice. Although we cannot fully exclude a subtle role of Frabin/Fgd4 in motor neurons that escaped our attention or species-specific differences in this context, our results suggest that the disease-initiating event in CMT4H is loss of a Schwann cell-specific cellular function of Frabin/Fgd4.

Frabin/Fgd4 function in Schwann cells is distinctively required in myelin maintenance

Establishing the PNS myelin sheath is a complex and expanded process, which roughly starts at birth and is completed in young

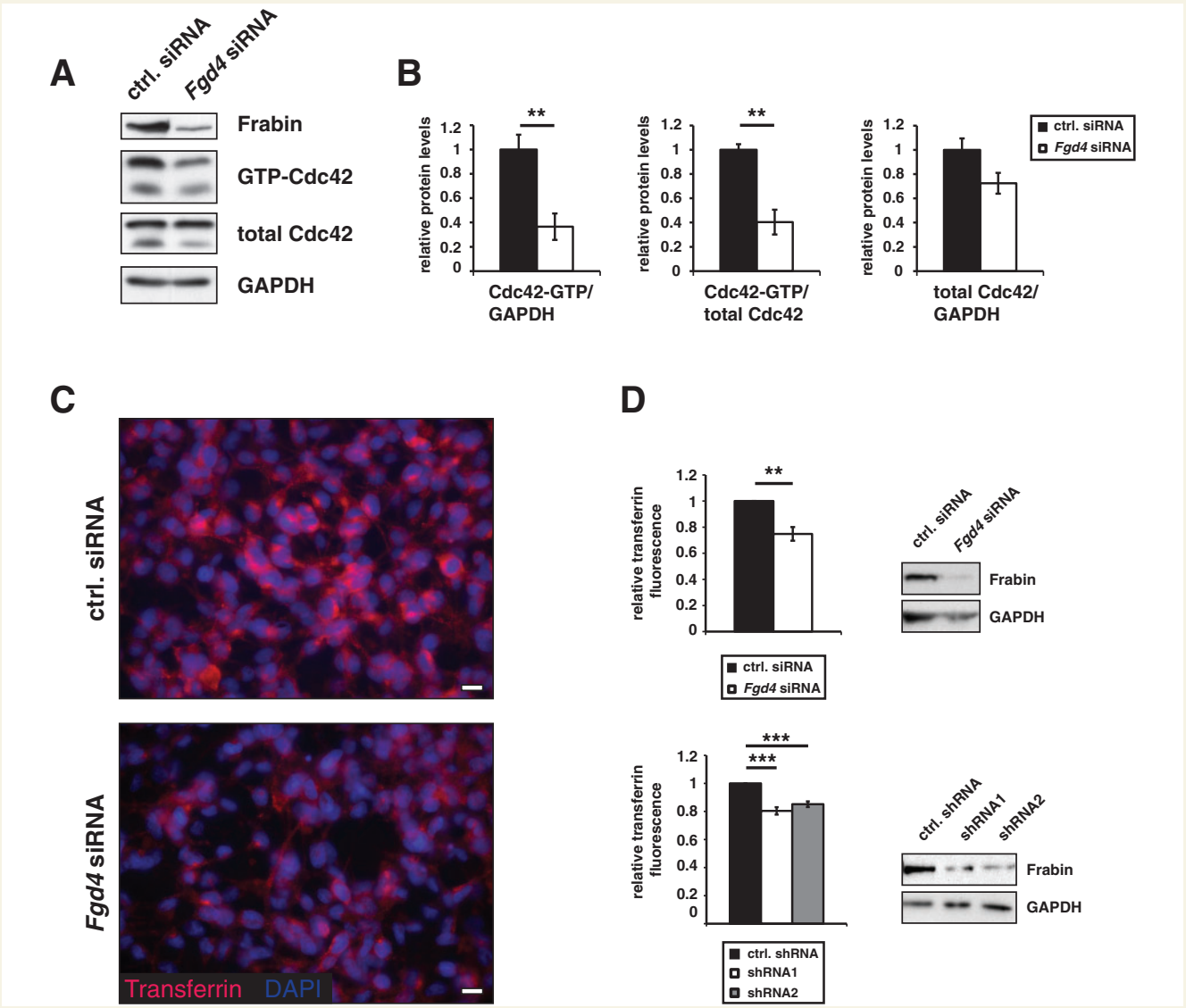

Figure 9 Knock-down of Frabin/Fgd4 leads to reduced activation of the RhoGTPase Cdc42 and impaired endocytosis. (**A** and **B**) Active, but not total levels of Cdc42 are significantly reduced in RT4 cells transfected with small interfering RNA (siRNA) targeting Frabin/Fgd4 in comparison with control-transfected cells. Four independent experiments were quantified. (**C**) Frabin/Fgd4-silenced RT4 cells qualitatively display reduced transferrin uptake ability compared with control-transfected cells. (**D**) Fluorescence activated cell sorting quantifications of Frabin/Fgd4-silenced RT4 cells reveal significant reductions in levels of incorporated transferrin. Transferrin fluorescence levels in cells transfected with small interfering RNA (*upper* panel) or short hairpin RNA (*lower* panel) targeting Frabin/Fgd4 were compared with transferrin fluorescence levels in cells transfected with control small interfering RNA or short hairpin RNA. Three independent experiments were quantified with small interfering RNA-transfected cells and four independent experiments with short hairpin RNA-transfected cells. Scale bars = 10 μm; $^{**}P < 0.01$; $^{***}P < 0.001$; Student's *t*-test (two-tailed). GADPH = glyceraldehyde-3-phosphate dehydrogenase.

adulthood (Jessen and Mirsky, 2005). CMT4H has an early onset and a slowly progressive course, attaining a severe clinical phenotype during the second half of life when myelination has long been completed. Thus, we asked whether Frabin/Fgd4 function is only necessary in development when the myelin sheath is being established. This pre-existing myelin defect would then passively aggravate during adulthood, leading to the observed progressive pathology, without requiring Frabin/Fgd4 function during myelin maintenance. Alternatively, Frabin/Fgd4 function may be actively required for both myelin development and maintenance. If true, lack of Frabin/Fgd4 function in the adult may also contribute to the progressive course of CMT4H. We addressed these mechanistically important questions using a mouse line that allows inducible Schwann cell-specific Frabin/Fgd4 deletion in adult animals. We found that loss of Frabin/Fgd4, induced in young adults when myelination was virtually completed, still resulted in histopathological myelin alterations as seen in $Fgd4^{-/-}$ animals and in CMT4H. Quantitative comparisons revealed only a slightly reduced number of affected fibres compared with age-matched constitutive $Fgd4^{-/-}$ mutants. We conclude that Frabin/Fgd4

function is not only required for correct developmental myelination but also specifically and prominently for myelin maintenance. Thus, one might speculate that a potential therapeutic approach based on reconstitution of Frabin/Fgd4 function in CMT4H might possibly work in adult individuals, as an active process requiring Frabin/Fgd4 in adult myelinating Schwann cells seems to be majorly impaired.

The Frabin–Cdc42 axis in Schwann cells and myelination

Frabin/Fgd4 is a member of the faciogenital dysplasia family of proteins and has been described as a GEF for RhoGTPases, in particular for Cdc42 (Nakanishi and Takai, 2008). The available evidence to support this claim is based mainly on the ability of Frabin/Fgd4 to activate downstream effectors of Cdc42, to influence cell morphology and to recruit Cdc42 to the plasma membrane, when Frabin/Fgd4 was overexpressed in cultured cells (Nakanishi and Takai, 2008). Furthermore, biochemical evidence for a GEF function of Frabin/Fgd4 on Cdc42 has been obtained in a cell-free system (Umikawa *et al.*, 1999). To examine the Frabin/Fgd4–Cdc42 axis in peripheral nerves more specifically, we measured active and total Cdc42 levels in sciatic nerve lysates from wild-type and *Fgd4*$^{-/-}$ mice. We found a substantial and significant reduction in active Cdc42 when Frabin/Fgd4 was absent, while total Cdc42 levels were not changed. These findings provide evidence for a functional link between Frabin/Fgd4 and active Cdc42 *in vivo* and further support GEF activity of Frabin/Fgd4 on Cdc42. Although we consider it unlikely, we cannot exclude contributions by indirect activation mechanisms. A definitive analysis would require direct *in vivo* measurements of specific GTP exchange rates in peripheral nerves. Currently, this procedure is technically not feasible. To further support our findings in other ways, we switched to cell culture. Both in Frabin/Fgd4-silenced RT4 cells and Frabin/Fgd4-silenced primary rat Schwann cells (data not shown), we found prominently reduced active levels of Cdc42 compared with control cells. These data are in agreement with our *in vivo* results and support the hypothesis that the key molecular function of Frabin/Fgd4 involves activation of Cdc42 in the context of crucial Schwann cell functions. Interestingly, a second GEF for RhoGTPases, ARHGEF10, has also been implicated in the control of myelination. A missense mutation associated with slowed nerve conduction velocity and thin PNS myelin sheaths was found (Verhoeven *et al.*, 2003). In contrast to Frabin/Fgd4 mutations, this mutant seems to act through hyperactivated GEF activity on RhoGTPases, in line with the dominant segregation of reduced nerve conduction velocity within the ARHGEF10 mutation-carrying family (Chaya *et al.*, 2011).

Our data support the hypothesis that the initial trigger in CMT4H is loss of Frabin/Fdg4 in Schwann cells. Frabin/Fgd4 function is still actively required to maintain a correctly structured myelin sheath in the adult and is paralleled by reduced active levels of Cdc42. Indeed, we show that eliminating Cdc42 from adult myelinating Schwann cells phenocopies the consequences of loss of Frabin/Fgd4. These experiments further strengthen the argument for a critical connection between Frabin/Fgd4 and Cdc42 in the PNS throughout life and demonstrate that Cdc42 is required for myelin maintenance, in addition to the critical role of this RhoGTPase and associated signalling pathways in developmental myelination (Benninger *et al.*, 2007; Pereira *et al.*, 2012). Taken together, these results provide strong evidence that the reduction in active Cdc42 levels is at least contributing to the pathology of CMT4H.

In our quest to understand the cellular consequences of the functional link between Frabin/Fgd4 and Cdc42 in Schwann cell biology, we faced the extraordinary pleiotropy of Cdc42 function (Etienne-Manneville and Hall, 2002; Jaffe and Hall, 2005; Melendez *et al.*, 2011). Specificity in cellular function is reached by strict regulation of Cdc42 activity, and GEFs play a decisive role in this regulatory process. They recruit and activate Cdc42 at specific subcellular locations, therefore exerting distinct mechanistic influences on Cdc42 effectors, which finally results in particular cellular functions (Garcia-Mata and Burridge, 2007). For example, the faciogenital dysplasia family member Fgd1, which is mutated in Aarskog–Scott syndrome, a rare X-linked disorder characterized by typical facial dysmorphism and skeletal and genital anomalies (Pasteris *et al.*, 1994), is involved in Cdc42-dependent processes, such as cell migration (Oshima *et al.*, 2011), vesicular transport (Egorov *et al.*, 2009) and podosome formation (Daubon *et al.*, 2011). Similarly, Fgd2 has been linked to Cdc42-dependent vesicle trafficking (Huber *et al.*, 2008), and Fgd3 influences cell motility and cellular morphology in a Cdc42-dependent manner (Hayakawa *et al.*, 2008). Moreover, a unique clinical form of Charcot–Marie–Tooth disease with glomerulopathy results from specific allelic variants of inverted formin 2 (Boyer *et al.*, 2011). This formin protein interacts with Cdc42 and myelin and lymphocyte protein), implicated in proper myelination (Schaeren-Wiemers *et al.*, 2004; Buser *et al.*, 2009), suggesting that myelinopathy and glomerulopathy in this special form of Charcot–Marie–Tooth disease may represent particular dysfunction of cell types (Schwann cells and podocytes), both with specialized membrane biology. We reasoned that Frabin/Fgd4 might be involved in similar cellular processes and found that this GEF is required for efficient endocytosis. There is increasing evidence that endocytic transport is critical in myelination. Disturbed Rab11-dependent endocytic recycling is a potential disease mechanism for CMT4C (Lupo *et al.*, 2009; Roberts *et al.*, 2010; Stendel *et al.*, 2010) and dynamin 2 mutations, associated with dominant-intermediate Charcot–Marie–Tooth disease type B, cause disturbed clathrin-mediated endocytosis (Sidiropoulos *et al.*, 2012). Cdc42 is involved in endocytosis (Ridley, 2006; Doherty and McMahon, 2009) and most likely enables clathrin-mediated endocytosis (Yang *et al.*, 2001; Bu *et al.*, 2010; Shen *et al.*, 2011) by directed actin polymerization and therefore rearrangement of the actin cytoskeleton in the vicinity of clathrin-coated pits (Kaksonen *et al.*, 2006). We have observed co-localization of Frabin/Fgd4 and Cdc42 after overexpression in RT4 cells (data not shown), consistent with the hypothesis that Frabin/Fgd4 may be involved in recruiting and activating Cdc42 at the plasma membrane of Schwann cells, thereby contributing to the cellular process of endocytosis. Endocytosis is critical for the regulation of protein and lipid homeostasis in the plasma membrane and a defect in endocytosis may result in irregular accumulation of proteins and lipids at the plasma membrane. Thus, we suggest that altered myelin membrane dynamics may contribute

to the myelin pathology observed in Frabin/Fgd4-mutant mice and in CMT4H. Alternatively, receptor molecules may accumulate on the cellular surface resulting in altered cellular signalling, which could be, at least partially, responsible for the observed CMT4H pathology. Nevertheless, given the broad spectrum of functions of Cdc42, other Cdc42-dependent cellular processes are likely to be also involved in CMT4H.

Convergent and divergent signalling pathways and the formation of redundant myelin folds

Some autosomal recessive demyelinating forms of Charcot–Marie–Tooth disease, most prominently CMT4B, CMT4H and to a minor degree CMT4F (culprit gene periaxin; Boerkoel *et al.*, 2001; Takashima *et al.*, 2002; Marchesi *et al.*, 2010), are characterized by comparable histopathological features, including myelin thickenings, redundant myelin loops (focally folded myelin with tomacula formation, a characteristic feature also found in hereditary neuropathy with liability to pressure palsy; Suter and Scherer, 2003) and myelin infoldings and outfoldings (Nave *et al.*, 2007). Interestingly, when analysing myelin thickness in animal models for CMT4B and CMT4H, no altered growth ratio of unaffected fibres (fibres without histopathological features) was detected (Bonneick *et al.*, 2005; Tersar *et al.*, 2007; this study). These findings indicate that the neuropathological features in these animal models do not reflect a major overshooting in radial growth of myelin, but rather a lateral surplus of myelin. The observed excess of myelin seemed to arise mainly in the neighbourhood of nodes of Ranvier and Schmidt–Lanterman incisures where the main addition of myelin is thought to occur. This speculation based on histological results raises the question of how a possible lateral surplus of myelin occurs. One possible answer to this question consists in the perspective of persisting myelin growth over the normal level. Myelination in the PNS is stimulated by axonal neuregulin-1 type III through mainly PI3Kinase/AKT and extracellular-signal regulated kinase/mitogen-activated protein kinase signalling (Pereira *et al.*, 2012). Accordingly, mice with myelinating glia-specific loss of PTEN, a lipid phosphatase that inhibits AKT signalling, exhibit mammalian target for rapamycin-dependent overmyelination (Goebbels *et al.*, 2010, 2012). Furthermore, interactions between mammalian Dlg1 and PTEN are required for the stabilization of PTEN acting as myelination brake in Schwann cells to prevent AKT-dependent overmyelination (Cotter *et al.*, 2010). In the PNS of Myotubularin-related protein-2$^{-/-}$ mice, the absence of this myelination brake attained by reduction in Dlg1 levels has been suggested to be causative for the observed pathological over-myelination phenotype (Cotter *et al.*, 2010). In our analysis of *Fgd4*$^{-/-}$ mice, we did not detect hyperactivation of known myelination-driving pathways. Provided that these results are not because of transient- or low-signal phenomena that escaped detection, we favour the hypothesis that there is molecular heterogeneity in the different pathways leading to hypermyelination, in particular in those cases where aberrant myelin folds are observed. Given the virtual identical pathology in CMT4H and CMT4B, phosphoinositide signalling pathways that are not immediately linked to AKT regulation need to be considered (Suter, 2007). Frabin/Fgd4 contains a FYVE (Fab1, YOTB, Vac1 and EEA1) and two pleckstrin homology domains that most likely bind to phophoinositides, suggesting potential cooperation with the CMT4B culprits Myotubularin-related protein-2 and Myotubularin-related protein-13/Set-binding factor-2, which regulate synthesis of specific phosphoinositides (Hnia *et al.*, 2012) as does the CMT4J culprit protein FIG4 (Chow *et al.*, 2007).

Conclusions

With the generation and characterization of an animal model for CMT4H, we show that loss of Frabin/Fgd4 causes a recessive, distally pronounced, demyelinating peripheral neuropathy with early onset and progressive course. In addition, we have provided novel insights into cellular and molecular mechanisms altered in CMT4H. This knowledge sets a firm basis to dissect the underlying disease mechanisms further, to elucidate common and divergent pathways leading to hereditary neuropathies, and eventually to provide hints as to novel molecularly targeted treatment strategies.

Acknowledgements

The authors thank the members of the Suter lab for many fruitful discussions, S. Arber for Hb9-Cre mice and D. Meijer for Dhh-Cre mice, J. Collard for reagents and R. Martini for advice. The authors are also grateful for the support from the Electron Microscopy Center of the ETH Zurich and acknowledge the generation of Frabin/Fgd4 mutant mice by the Mouse Clinical Institute (Strasbourg, France).

Funding

The Swiss National Science Foundation and the National Centre of Competence in Research (NCCR), Neural Plasticity and Repair (to U.S.); Research funds of the University of Würzburg Medical Center (to C.W. and K.V.T.); The Deutsche Forschungsgemeinschaft (SE 1839/1-1 to J.S.).

Supplementary material

Supplementary material is available at *Brain* online.

References

Arber S, Han B, Mendelsohn M, Smith M, Jessell TM, Sockanathan S. Requirement for the homeobox gene Hb9 in the consolidation of motor neuron identity. Neuron 1999; 23: 659–74.

Azzedine H, Bolino A, Taieb T, Birouk N, Di Duca M, Bouhouche A, et al. Mutations in MTMR13, a new pseudophosphatase homologue of MTMR2 and Sbf1, in two families with an autosomal recessive demyelinating form of Charcot-Marie-Tooth disease associated with early-onset glaucoma. Am J Hum Genet 2003; 72: 1141–53.

Baets J, Deconinck T, De Vriendt E, Zimon M, Yperzeele L, Van Hoorenbeeck K, et al. Genetic spectrum of hereditary neuropathies with onset in the first year of life. Brain 2011; 134: 2664–76.

Benninger Y, Thurnherr T, Pereira JA, Krause S, Wu X, Chrostek-Grashoff A, et al. Essential and distinct roles for cdc42 and rac1 in the regulation of Schwann cell biology during peripheral nervous system development. J Cell Biol 2007; 177: 1051–61.

Boerkoel CF, Takashima H, Stankiewicz P, Garcia CA, Leber SM, Rhee-Morris L, et al. Periaxin mutations cause recessive Dejerine-Sottas neuropathy. Am J Hum Genet 2001; 68: 325–33.

Bolino A, Bolis A, Previtali SC, Dina G, Bussini S, Dati G, et al. Disruption of Mtmr2 produces CMT4B1-like neuropathy with myelin outfolding and impaired spermatogenesis. J Cell Biol 2004; 167: 711–21.

Bolino A, Muglia M, Conforti FL, LeGuern E, Salih MA, Georgiou DM, et al. Charcot-Marie-Tooth type 4B is caused by mutations in the gene encoding myotubularin-related protein-2. Nat Genet 2000; 25: 17–19.

Bonneick S, Boentert M, Berger P, Atanasoski S, Mantei N, Wessig C, et al. An animal model for Charcot-Marie-Tooth disease type 4B1. Hum Mol Genet 2005; 14: 3685–95.

Boyer O, Nevo F, Plaisier E, Funalot B, Gribouval O, Benoit G, et al. INF2 mutations in Charcot-Marie-Tooth disease with glomerulopathy. N Engl J Med 2011; 365: 2377–88.

Bremer J, Baumann F, Tiberi C, Wessig C, Fischer H, Schwarz P, et al. Axonal prion protein is required for peripheral myelin maintenance. Nat Neurosci 2010; 13: 310–18.

Bu W, Lim KB, Yu YH, Chou AM, Sudhaharan T, Ahmed S. Cdc42 interaction with N-WASP and Toca-1 regulates membrane tubulation, vesicle formation and vesicle motility: implications for endocytosis. PLoS One 2010; 5: e12153.

Buser AM, Schmid D, Kern F, Erne B, Lazzati T, Schaeren-Wiemers N. The myelin protein MAL affects peripheral nerve myelination: a new player influencing p75 neurotrophin receptor expression. Eur J Neurosci 2009; 29: 2276–90.

Chaya T, Shibata S, Tokuhara Y, Yamaguchi W, Matsumoto H, Kawahara I, et al. Identification of a negative regulatory region for the exchange activity and characterization of T332I mutant of Rho guanine nucleotide exchange factor 10 (ARHGEF10). J Biol Chem 2011; 286: 29511–20.

Chow CY, Zhang Y, Dowling JJ, Jin N, Adamska M, Shiga K, et al. Mutation of FIG4 causes neurodegeneration in the pale tremor mouse and patients with CMT4J. Nature 2007; 448: 68–72.

Cotter L, Ozcelik M, Jacob C, Pereira JA, Locher V, Baumann R, et al. Dlg1-PTEN interaction regulates myelin thickness to prevent damaging peripheral nerve overmyelination. Science 2010; 328: 1415–18.

Daubon T, Buccione R, Genot E. The Aarskog-Scott syndrome protein Fgd1 regulates podosome formation and extracellular matrix remodeling in transforming growth factor beta-stimulated aortic endothelial cells. Mol Cell Biol 2011; 31: 4430–41.

De Sandre-Giovannoli A, Delague V, Hamadouche T, Chaouch M, Krahn M, Boccaccio I, et al. Homozygosity mapping of autosomal recessive demyelinating Charcot-Marie-Tooth neuropathy (CMT4H) to a novel locus on chromosome 12p11.21-q13.11. J Med Genet 2005; 42: 260–5.

Delague V, Jacquier A, Hamadouche T, Poitelon Y, Baudot C, Boccaccio I, et al. Mutations in FGD4 encoding the Rho GDP/GTP exchange factor FRABIN cause autosomal recessive Charcot-Marie-Tooth type 4H. Am J Hum Genet 2007; 81: 1–16.

Doherty GJ, McMahon HT. Mechanisms of endocytosis. Annu Rev Biochem 2009; 78: 857–902.

Egorov MV, Capestrano M, Vorontsova OA, Di Pentima A, Egorova AV, Mariggio S, et al. Faciogenital dysplasia protein (FGD1) regulates export of cargo proteins from the golgi complex via Cdc42 activation. Mol Biol Cell 2009; 20: 2413–27.

Etienne-Manneville S, Hall A. Rho GTPases in cell biology. Nature 2002; 420: 629–35.

Fabrizi GM, Taioli F, Cavallaro T, Ferrari S, Bertolasi L, Casarotto M, et al. Further evidence that mutations in FGD4/frabin cause Charcot-Marie-Tooth disease type 4H. Neurology 2009; 72: 1160–4.

Fledrich R, Schlotter-Weigel B, Schnizer TJ, Wichert SP, Stassart RM, zu Horste GM, et al. A rat model of Charcot-Marie-Tooth disease 1A recapitulates disease variability and supplies biomarkers of axonal loss in patients. Brain 2012a; 135: 72–87.

Fledrich R, Stassart RM, Sereda MW. Murine therapeutic models for Charcot-Marie-Tooth (CMT) disease. Br Med Bull 2012b; 102: 89–113.

Frei R, Motzing S, Kinkelin I, Schachner M, Koltzenburg M, Martini R. Loss of distal axons and sensory Merkel cells and features indicative of muscle denervation in hindlimbs of P0-deficient mice. J Neurosci 1999; 19: 6058–67.

Garcia-Mata R, Burridge K. Catching a GEF by its tail. Trends Cell Biol 2007; 17: 36–43.

Goebbels S, Oltrogge JH, Kemper R, Heilmann I, Bormuth I, Wolfer S, et al. Elevated phosphatidylinositol 3,4,5-trisphosphate in glia triggers cell-autonomous membrane wrapping and myelination. J Neurosci 2010; 30: 8953–64.

Goebbels S, Oltrogge JH, Wolfer S, Wieser GL, Nientiedt T, Pieper A, et al. Genetic disruption of Pten in a novel mouse model of tomaculous neuropathy. EMBO Mol Med 2012; 4: 486–99.

Hayakawa M, Matsushima M, Hagiwara H, Oshima T, Fujino T, Ando K, et al. Novel insights into FGD3, a putative GEF for Cdc42, that undergoes SCF(FWD1/beta-TrCP)-mediated proteasomal degradation analogous to that of its homologue FGD1 but regulates cell morphology and motility differently from FGD1. Genes Cells 2008; 13: 329–42.

Hnia K, Vaccari I, Bolino A, Laporte J. Myotubularin phosphoinositide phosphatases: cellular functions and disease pathophysiology. Trends Mol Med 2012; 18: 317–27.

Houlden H, Hammans S, Katifi H, Reilly MM. A novel Frabin (FGD4) nonsense mutation p.R275X associated with phenotypic variability in CMT4H. Neurology 2009; 72: 617–20.

Huber C, Martensson A, Bokoch GM, Nemazee D, Gavin AL. FGD2, a CDC42-specific exchange factor expressed by antigen-presenting cells, localizes to early endosomes and active membrane ruffles. J Biol Chem 2008; 283: 34002–12.

Jaegle M, Ghazvini M, Mandemakers W, Piirsoo M, Driegen S, Levavasseur F, et al. The POU proteins Brn-2 and Oct-6 share important functions in Schwann cell development. Genes Dev 2003; 17: 1380–91.

Jaffe AB, Hall A. Rho GTPases: biochemistry and biology. Annu Rev Cell Dev Biol 2005; 21: 247–69.

Jessen KR, Mirsky R. The origin and development of glial cells in peripheral nerves. Nat Rev Neurosci 2005; 6: 671–82.

Kaksonen M, Toret CP, Drubin DG. Harnessing actin dynamics for clathrin-mediated endocytosis. Nat Rev Mol Cell Biol 2006; 7: 404–14.

Krajewski KM, Lewis RA, Fuerst DR, Turansky C, Hinderer SR, Garbern J, et al. Neurological dysfunction and axonal degeneration in Charcot-Marie-Tooth disease type 1A. Brain 2000; 123: 1516–27.

Leone DP, Genoud S, Atanasoski S, Grausenburger R, Berger P, Metzger D, et al. Tamoxifen-inducible glia-specific Cre mice for somatic mutagenesis in oligodendrocytes and Schwann cells. Mol Cell Neurosci 2003; 22: 430–40.

Lupo V, Galindo MI, Martinez-Rubio D, Sevilla T, Vilchez JJ, Palau F, et al. Missense mutations in the SH3TC2 protein causing Charcot-Marie-Tooth disease type 4C affect its localization in the plasma membrane and endocytic pathway. Hum Mol Genet 2009; 18: 4603–14.

Marchesi C, Milani M, Morbin M, Cesani M, Lauria G, Scaioli V, et al. Four novel cases of periaxin-related neuropathy and review of the literature. Neurology 2010; 75: 1830–8.

Martini R. Animal models for inherited peripheral neuropathies: chances to find treatment strategies? J Neurosci Res 2000; 61: 244–50.

Melendez J, Grogg M, Zheng Y. Signaling role of Cdc42 in regulating mammalian physiology. J Biol Chem 2011; 286: 2375–81.

Nakanishi H, Takai Y. Frabin and other related Cdc42-specific guanine nucleotide exchange factors couple the actin cytoskeleton with the plasma membrane. J Cell Mol Med 2008; 12: 1169–76.

Nave KA. Myelination and support of axonal integrity by glia. Nature 2010; 468: 244–52.

Nave KA, Sereda MW, Ehrenreich H. Mechanisms of disease: inherited demyelinating neuropathies—from basic to clinical research. Nat Clin Pract Neurol 2007; 3: 453–64.

Nave KA, Trapp BD. Axon-glial signaling and the glial support of axon function. Annu Rev Neurosci 2008; 31: 535–61.

Nicholson G, Myers S. Intermediate forms of Charcot-Marie-Tooth neuropathy: a review. Neuromolecular Med 2006; 8: 123–30.

Oshima T, Fujino T, Ando K, Hayakawa M. Role of FGD1, a Cdc42 guanine nucleotide exchange factor, in epidermal growth factor-stimulated c-Jun NH2-terminal kinase activation and cell migration. Biol Pharm Bull 2011; 34: 54–60.

Ozcelik M, Cotter L, Jacob C, Pereira JA, Relvas JB, Suter U, et al. Pals1 is a major regulator of the epithelial-like polarization and the extension of the myelin sheath in peripheral nerves. J Neurosci 2010; 30: 4120–31.

Pasteris NG, Cadle A, Logie LJ, Porteous ME, Schwartz CE, Stevenson RE, et al. Isolation and characterization of the faciogenital dysplasia (Aarskog-Scott syndrome) gene: a putative Rho/Rac guanine nucleotide exchange factor. Cell 1994; 79: 669–78.

Pereira JA, Baumann R, Norrmen C, Somandin C, Miehe M, Jacob C, et al. Dicer in Schwann cells is required for myelination and axonal integrity. J Neurosci 2010; 30: 6763–75.

Pereira JA, Benninger Y, Baumann R, Goncalves AF, Ozcelik M, Thurnherr T, et al. Integrin-linked kinase is required for radial sorting of axons and Schwann cell remyelination in the peripheral nervous system. J Cell Biol 2009; 185: 147–61.

Pereira JA, Lebrun-Julien F, Suter U. Molecular mechanisms regulating myelination in the peripheral nervous system. Trends Neurosci 2012; 35: 123–34.

Reilly MM, Murphy SM, Laura M. Charcot-Marie-Tooth disease. J Peripher Nerv Syst 2011; 16: 1–14.

Ridley AJ. Rho GTPases and actin dynamics in membrane protrusions and vesicle trafficking. Trends Cell Biol 2006; 16: 522–9.

Roberts RC, Peden AA, Buss F, Bright NA, Latouche M, Reilly MM, et al. Mistargeting of SH3TC2 away from the recycling endosome causes Charcot-Marie-Tooth disease type 4C. Hum Mol Genet 2010; 19: 1009–18.

Robinson FL, Niesman IR, Beiswenger KK, Dixon JE. Loss of the inactive myotubularin-related phosphatase Mtmr13 leads to a Charcot-Marie-Tooth 4B2-like peripheral neuropathy in mice. Proc Natl Acad Sci USA 2008; 105: 4916–21.

Rogers DC, Fisher EM, Brown SD, Peters J, Hunter AJ, Martin JE. Behavioral and functional analysis of mouse phenotype: SHIRPA, a proposed protocol for comprehensive phenotype assessment. Mamm Genome 1997; 8: 711–13.

Salzer JL. Switching myelination on and off. J Cell Biol 2008; 181: 575–7.

Sander EE, van Delft S, ten Klooster JP, Reid T, van der Kammen RA, Michiels F, et al. Matrix-dependent Tiam1/Rac signaling in epithelial cells promotes either cell-cell adhesion or cell migration and is regulated by phosphatidylinositol 3-kinase. J Cell Biol 1998; 143: 1385–98.

Schaeren-Wiemers N, Bonnet A, Erb M, Erne B, Bartsch U, Kern F, et al. The raft-associated protein MAL is required for maintenance of proper axon–glia interactions in the central nervous system. J Cell Biol 2004; 166: 731–42.

Senderek J, Bergmann C, Weber S, Ketelsen UP, Schorle H, Rudnik-Schoneborn S, et al. Mutation of the SBF2 gene, encoding a novel member of the myotubularin family, in Charcot-Marie-Tooth neuropathy type 4B2/11p15. Hum Mol Genet 2003; 12: 349–56.

Shen H, Ferguson SM, Dephoure N, Park R, Yang Y, Volpicelli-Daley L, et al. Constitutive activated Cdc42-associated kinase (Ack) phosphorylation at arrested endocytic clathrin-coated pits of cells that lack dynamin. Mol Biol Cell 2011; 22: 493–502.

Shy ME, Lupski JR, Chance PF, Klein CJ, Dyck PJ. Hereditary motor and sensory neuropathies: an overview of clinical, genetic, electrophysiologic, and pathologic features. In: Dyck PJ, Thomas PK, editors. Peripheral neuropathy. Philadelphia: Elsevier Saunders; 2005. p. 1623–58.

Sidiropoulos PN, Miehe M, Bock T, Tinelli E, Oertli CI, Kuner R, et al. Dynamin 2 mutations in Charcot-Marie-Tooth neuropathy highlight the importance of clathrin-mediated endocytosis in myelination. Brain 2012; 135: 1395–411.

Skre H. Genetic and clinical aspects of Charcot-Marie-Tooth's disease. Clin Genet 1974; 6: 98–118.

Somandin C, Gerber D, Pereira JA, Horn M, Suter U. LITAF (SIMPLE) regulates Wallerian degeneration after injury but is not essential for peripheral nerve development and maintenance: Implications for Charcot-Marie-Tooth disease. Glia 2012; 60: 1518–28.

Stendel C, Roos A, Deconinck T, Pereira J, Castagner F, Niemann A, et al. Peripheral nerve demyelination caused by a mutant Rho GTPase guanine nucleotide exchange factor, frabin/FGD4. Am J Hum Genet 2007; 81: 158–64.

Stendel C, Roos A, Kleine H, Arnaud E, Ozcelik M, Sidiropoulos PN, et al. SH3TC2, a protein mutant in Charcot-Marie-Tooth neuropathy, links peripheral nerve myelination to endosomal recycling. Brain 2010; 133: 2462–74.

Suter U. Phosphoinositides and Charcot-Marie-tooth disease: new keys to old questions. Cell Mol Life Sci 2007; 64: 3261–5.

Suter U, Nave KA. Transgenic mouse models of CMT1A and HNPP. Ann N Y Acad Sci 1999; 883: 247–53.

Suter U, Scherer SS. Disease mechanisms in inherited neuropathies. Nat Rev Neurosci 2003; 4: 714–26.

Takashima H, Boerkoel CF, De Jonghe P, Ceuterick C, Martin JJ, Voit T, et al. Periaxin mutations cause a broad spectrum of demyelinating neuropathies. Ann Neurol 2002; 51: 709–15.

Taveggia C, Feltri ML, Wrabetz L. Signals to promote myelin formation and repair. Nat Rev Neurol 2010; 6: 276–87.

Tersar K, Boentert M, Berger P, Bonneick S, Wessig C, Toyka KV, et al. Mtmr13/Sbf2-deficient mice: an animal model for CMT4B2. Hum Mol Genet 2007; 16: 2991–3001.

Thurnherr T, Benninger Y, Wu X, Chrostek A, Krause SM, Nave KA, et al. Cdc42 and Rac1 signaling are both required for and act synergistically in the correct formation of myelin sheaths in the CNS. J Neurosci 2006; 26: 10110–19.

Umikawa M, Obaishi H, Nakanishi H, Satoh-Horikawa K, Takahashi K, Hotta I, et al. Association of frabin with the actin cytoskeleton is essential for microspike formation through activation of Cdc42 small G protein. J Biol Chem 1999; 274: 25197–200.

Verhoeven K, De Jonghe P, Van de Putte T, Nelis E, Zwijsen A, Verpoorten N, et al. Slowed conduction and thin myelination of peripheral nerves associated with mutant rho Guanine-nucleotide exchange factor 10. Am J Hum Genet 2003; 73: 926–32.

Wu X, Quondamatteo F, Lefever T, Czuchra A, Meyer H, Chrostek A, et al. Cdc42 controls progenitor cell differentiation and beta-catenin turnover in skin. Genes Dev 2006; 20: 571–85.

Yang W, Lo CG, Dispenza T, Cerione RA. The Cdc42 target ACK2 directly interacts with clathrin and influences clathrin assembly. J Biol Chem 2001; 276: 17468–73.

Zielasek J, Martini R, Toyka KV. Functional abnormalities in P0-deficient mice resemble human hereditary neuropathies linked to P0 gene mutations. Muscle Nerve 1996; 19: 946–52.